Environmental Pollution 281 (2021) 117012

Contents lists available at ScienceDirect

Environmental Pollution

journal homepage: www.elsevier.com/locate/envpol

Microbial transformation of biogenic and abiogenic Fe minerals followed by in-situ incubations in an As-contaminated vs. non-contaminated aquifer

Martyna Glodowska [a, b, c, *], Magnus Schneider [d], Elisabeth Eiche [d], Agnes Kontny [d], Thomas Neumann [e], Daniel Straub [b, f], AdvectAs project members[1], Sara Kleindienst [b], Andreas Kappler [a]

[a] Geomicrobiology, Center for Applied Geosciences, University of Tübingen, Germany
[b] Microbial Ecology, Center for Applied Geosciences, University of Tübingen, Germany
[c] Department of Microbiology, IWWR, Radboud University, the Netherlands
[d] Karlsruhe Institute of Technology, Institute of Applied Geosciences, KIT, Germany
[e] Technical University of Berlin, Institute for Applied Geosciences, Berlin, Germany
[f] Quantitative Biology Center (QBiC), University of Tübingen, Germany

ARTICLE INFO

Article history:
Received 27 January 2021
Received in revised form
16 March 2021
Accepted 20 March 2021
Available online 26 March 2021

Keywords:
biogenic minerals
iron minerals
Fe(III) reduction
Fe(III) reducing bacteria
arsenic

ABSTRACT

Fe(III) minerals play a crucial role for arsenic (As) mobility in aquifers as they usually represent the main As-bearing phases. Microbial reductive dissolution of As-bearing Fe(III) minerals is responsible for the release of As and the resulting groundwater contamination in many sites worldwide. So far, in most studies mainly abiogenic iron minerals have been considered. Yet, biogenic minerals that possess different properties to their abiogenic counterparts are also present in the environment. In some environments they dominate the iron mineral inventory but so far, it is unclear what this means for the As mobility. We, therefore, performed an in-situ aquifer Fe(III) minerals exposure experiment i) to evaluate how different biogenic and abiogenic Fe(III) minerals are transformed in a strongly reducing, As-contaminated aquifer (25 m) compared to As-free moderately reducing aquifer (32 m) and ii) to assess which microbial taxa are involved in these Fe(III) minerals transformations. We found that higher numbers of bacteria and archaea were associated with the minerals incubated in the As-contaminated compared to the non-contaminated aquifer and that all Fe(III) minerals were mainly colonized by Fe(III)-reducing bacteria, with *Geobacter* being the most abundant taxon. Additionally, fermenting microorganisms were abundant on minerals incubated in the As-contaminated aquifer, while methanotrophs were identified on the minerals incubated in the As-free moderately reducing aquifer, implying involvement of these microorganisms in Fe(III) reduction. We observed that biogenic Fe(III) minerals generally tend to become more reduced and when incubated in the As-contaminated aquifer sorbed more As than the abiogenic ones. Most of abiogenic and biogenic Fe(III) minerals were transformed into magnetite while biogenic more crystalline mixed phases were not subjected to visible transformation. This in-situ Fe(III) minerals incubation approach shows that biogenic minerals are more prone to be colonized by (Fe(III)-reducing) microorganisms and bind more As, although ultimately produce similar minerals during Fe(III) reduction.

1. Introduction

Exposure to arsenic (As) is considered a major public health concern due to its toxic effect on human health and its carcinogenic potential (National Research Council, 2001). Although As contaminates mainly surface water and groundwater, it ultimately enters the food chain as the water is used for cooking and drinking, while

* Corresponding author. Department of Microbiology, IWWR, Radboud University, the Netherlands.
E-mail address: m.glodowska@science.ru.nl (M. Glodowska).
[1] AdvectAs Project Members—listed in the SI

https://doi.org/10.1016/j.envpol.2021.117012

anoxic conditions in rice paddy soil lead to the release of As and its accumulation in crops. (Arain et al., 2009; Molin et al., 2015; Muhammad et al., 2010). Since As does not change the color, smell or taste of water and food, it is very difficult to detect its presence without expensive and time-consuming analysis. In consequence, many people have been chronically consuming this toxic metalloid for decades. This is particularly alarming as recent studies have shown that up to 220 million people worldwide are potentially exposed to elevated As concentrations in groundwater, overpassing the WHO limit of 10 μg/L (Podgorski and Berg, 2020). What is even more concerning, the majority of affected areas (94%), where As concentrations were likely to exceed 10 μg/L, were identified in the most populated regions of Asia. Despite a substantial increase of awareness regarding the potential risks associated with consumption of As-contaminated water, many people from rural affected areas simply have no access to safe water or cannot afford commercially available filters for water purification. Consequently, As poisoning still remains a global health threat, particularly in the highly affected areas of South and Southeast Asia.

Although As is an element with minor abundance and an average concentration of 1.5–3 mg/kg in the continental crust, it is the 20th most abundant element in the Earth's crust (Mandal and Suzuki, 2002) and it is broadly distributed in the environment (Lenoble et al., 2004). It was demonstrated that complete mobilization of As in amounts as small as 1 mg/kg from sandy Bangladesh aquifer sediment would increase the As groundwater concentration to an extreme value of 7950 μg/L (BGS and DPHE, 2001). Previous research has shown the importance of iron (Fe) minerals, mainly Fe(III) (oxyhydr)oxides, as main hosting phases for inorganic As, responsible for As immobilization within sediments (Kontny et al., 2021; Muehe and Kappler, 2014; Smedley and Kinniburgh, 2002; Welch et al., 2000). This is very important because on the one hand, adsorption of As by Fe(III) (oxyhydr)oxides is considered the main factor controlling As concentrations in the groundwater of many aquifers (Stollenwerk et al., 2007). On the other hand, one of the most commonly accepted mechanisms of As mobilization from sediments to groundwater is via microbially mediated reductive dissolution of As-bearing Fe(III) minerals (Chatain et al., 2005; Dhar et al., 2011; Islam et al., 2004; Neumann et al., 2014; Oremland and Stolz, 2003). Several previous studies have investigated As sorption capacities of various Fe(III) minerals (e.g., Ona-Nguema et al., 2005). In particular, high surface area, poorly crystalline Fe(III) phases such as ferrihydrite (Fh) have a high affinity toward As. Yet, these poorly crystalline Fe(III) phases are known to be less stable and more bioavailable as they are preferentially exploited by Fe(III)-reducing microorganisms as terminal electron acceptor (Lovley et al., 1991). Therefore, although these poorly crystalline Fe(III) minerals may sorb more As, they tend to more easily release it under strongly reducing conditions (Neidhardt et al., 2018).

The high surface area and strong affinity towards metals and metalloids make Fe(III) minerals an effective sorbent for the removal of toxic metals from water (Bakatula et al., 2016), and thus an effective water remediation strategy (Petrusevski et al., 2007). In consequence, a lot of attention focused on quantifying As sorption onto different Fe(III) minerals. However, the vast majority of studies used abiogenic or synthetic minerals (Dixit and Hering, 2003; Farquhar et al., 2002; Gimenez et al., 2007; Manning et al., 1998). Very little work has been done using biogenic Fe(III) minerals which are produced by microbial activity, either as external or internal precipitates (Ferris, 2005; Fortin and Langley, 2005; Hao et al., 2016; Kleinert et al., 2011; Muehe et al., 2016).

This is surprising as microbially driven processes are an integral part of Fe cycling, contributing to Fe(III) reduction but also to Fe(II) oxidation and subsequent biogenic Fe(III) mineral formation (Kappler et al., 2021; Posth et al., 2014). Minerals formed as a result of direct metabolic activity of bacteria usually occur as nanoparticles or small crystals (2–500 nm) and contain impurities such as sorbed or co-precipitated Si-ions, PO_4^{3-}, SO_4^{2-}, but also cations such as $Mn^{2+/4+}$, Al^{3+}, etc. (Fortin and Langley, 2005). Additionally, these biominerals may contain cell-derived organic matter (CDOM), and therefore overall possess different properties compared to their abiogenic counterparts (Hegler et al., 2008; Muehe et al., 2013b; Posth et al., 2010; Schädler et al., 2009). Nevertheless, biogenic Fe(III) minerals are present in nature and have been found across different environments (Abramov et al., 2020; Emerson et al., 1999; Fortin et al., 1998; Ueshima and Tazaki, 2001). Yet, a limited number of studies has been done using biogenic Fe(III) minerals which is likely related to the difficulty to synthesize them and the small amounts of minerals that can be biosynthesized in laboratory setups compared to abiogenic approaches. A few previous studies have investigated the role of biogenic Fe(III) minerals in the context of As sorption in the laboratory (Hohmann et al., 2010; Kleinert et al., 2011; Muehe et al., 2016). However, there is still a lack of knowledge when it comes to their bioavailability, their efficiency in As sorption compared to abiogenic minerals, their (trans)formation resulting from microbial reduction, and the microbial community that is involved in their transformation under environmental conditions. In order to address these knowledge gaps, we conducted an in-situ incubation experiment where we incubated a set of biogenic and abiogenic Fe(III) minerals in a moderately reducing As-free (32 m) and in a strongly reducing As-contaminated aquifer (25 m) in Vietnam.

2. Materials and methods

2.1. Study area

The study site is located in the village of Van Phuc, about 15 km SE from Hanoi city, Vietnam, on the banks of the Red River. Several studies have been conducted at this location, therefore extensive knowledge about the geology, mineralogy, hydrochemistry and microbiology is available (Berg et al., 2008; Eiche et al., 2008; Glodowska et al., 2020c; Kontny et al., 2021; Postma et al., 2017; Stopelli et al., 2020; van Geen et al., 2013; Wallis et al., 2020). In brief, the As-contaminated aquifer is of Holocene origin, characterized by strongly reducing conditions, high dissolved As (up to 513 μg/L), Fe (up to 20 mg/L) and CH_4 (up to 53 mg/L) concentrations. On the contrary, the moderately reducing low-As aquifer is of Pleistocene origin, which lies adjacent and underneath the Holocene aquifer, has low dissolved As (below 10 μg/L), very low Fe concentrations and not detectable CH_4. Between these two aquifers, a sharp transition zone characterized by changing redox conditions was found, where immobilization of As occurs. Due to the intensive groundwater abstraction in the Hanoi city area and surrounding municipals, a depression cone was formed that led to inversion of groundwater flow towards the Hanoi city center. As a consequence, As-contaminated groundwater from the Holocene aquifer is now flowing in the direction of the pristine Pleistocene aquifer threatening safe water supplies.

2.2. Abiogenic mineral synthesis and sand coating procedure

To coat the quartz (Qtz) grains with Fe minerals, synthetic Fe minerals (goethite (Gt)-Bayferrox 920, hematite (Hem)-Bayferrox 110, and magnetite (Mt)-Bayferro×360 with 0,3 μm particle size) from the company Lanxess/Bayferrox (LANXESS Inorganic Pigments, Krefeld, Germany) were used. All minerals have been tested with XRD (Bruker D8 Discover; see section 2.6) to ensure that the manufacturer's information is correct. The coating process followed

the procedure described previously (Hanna, 2007; Scheidegger et al., 1993; Schwertmann and Cornell, 2008). To obtain the coating solution, 100 mg of each mineral was mixed with 10 mL $NaNO_3$ solution in a 50 mL polyethylene tube and diluted with HNO_3 (sub-boiled) to adjust the desired pH. In order to obtain the maximum coating efficiency the ionic strength of the $NaNO_3$ solution was adjusted to 0.01 M and the pH to 7 for Gt (Schwertmann and Cornell, 2008), 5 for Mt (Hanna, 2007), and 2.5 for Hem (Schwertmann and Cornell, 2008). Afterwards the mineral suspensions were shaken at 25 °C for 24 h to obtain a homogeneous suspension. Before mixing with the Fe minerals, the sand was pretreated (washed) with 1.0 M HCl solution for 24 h, rinsed several times with distilled water and dried at 100 °C. 2.5 g of the acid-washed Qtz grains (0.4–0.8 mm, Roth) were added and the mineral-sand mixture was shaken for another 24 h.

The As content of all reaction components was quantified before the experiment. Inductively coupled plasma mass spectrometry (ICP-MS, X-Series 2, ThermoFisher) was used to analyse the initial $NaNO_3$ solution. The Qtz sand and the synthetic minerals were analyzed using energy dispersive X-ray fluorescence (ED-XRF). After the mineral coated sand settled, the supernatant was removed and the coated sand was washed several times with $NaNO_3$ solution with an ionic strength and pH equal to that of the reaction medium. Finally, the coated sand was washed free from any unattached Fe (oxyhydr)oxide first with a salt solution and then with pure water using a nylon sieve (63 μm). The samples with a pH above 5 (Gt, Mt) were additionally washed with 1 M $NaNO_3$ solution of pH 3 to remove weakly attached Fe (oxyhydr)oxide aggregates. The Gt-, Hem- and Mt-coated sand was finally dried in an oven at 110 °C for 24 h.

Abiogenic 2-line ferrihydrite (Fh) was synthetized following (Schwertmann and Cornell, 2008), directly in the presence of HCl-washed Qtz while shaking. The Fh-coated sand was left for 24 h at room temperature, afterwards washed with MilliQ water in order to remove any unattached Fe oxyhydroxide particles, and finally dried at 40 °C.

The geochemistry and mineralogy of the Fe-mineral coated sand grains was determined before and after the incubation experiment. For more details, see chapter 2.6.

2.3. Biogenic mineral synthesis and sand coating procedure

Biogenic Fh was prepared using the phototrophic Fe(II)-oxidizing bacterium *Rhodobacter ferrooxidans* sp. strain SW2 cultivated in low-phosphate medium containing 0.14 g KH_2PO_4, 0.2 NaCl, 0.3 g NH_4Cl, 0.5 g $MgSO_4$ x 7 H_2O, 0.1 g $CaCl_2$ x 2 H_2O, 1.85 g $NaHCO_3$ per 1 L of MilliQ water and pH adjusted to 7 (Kappler and Newman, 2004). Medium was prepared anoxically, transferred to 0.5 L Schott bottles and amended with anoxic solutions of 10 mM $FeCl_2$, 10 mM $NaNO_3$ and 5 mM acetate. Medium was left for 2 days in order to allow vivianite and siderite to precipitate. These minerals were removed by filtering the medium in the glovebox through 0.22 μm sterile vacuum filter (Millipore, Stericup™). In order to precipitate biogenic Fh directly on the sand, 10 g of HCl-washed and sterile sand was placed in 150 mL sterile serum bottles, amended with 100 mL of filtered medium, inoculated with 5% of SW2 culture, closed with a rubber stopper and crimped. All procedures were performed in the glovebox (100% N_2). The headspace of the serum bottles was exchanged with N_2/CO_2 atmosphere (8:2 ratio). Inoculated serum bottles were kept in horizontal position under constant light at 21 °C. Bottles were turned every day by hand within the first week to ensure homogeneous coating of the sand. At the end of Fe(II) oxidation, the medium was discarded from the serum bottle, and the Fh-coated sand was washed with anoxic MilliQ water several times in order to remove any unattached Fh and bacterial biomass, and subsequently dried at 40 °C.

Biogenic Gt was prepared using the nitrate-reducing Fe(II)-oxidizing bacterium *Acidovorax* sp. strain BoFeN1 (Kappler et al., 2005) and mineral medium containing 0.6 g KH_2PO_4, 0.3 g NH_4Cl, 0.5 g $MgSO_4$ x 7 H_2O, 0.1 g $CaCl_2$ x 2 H_2O and 1.85 g $NaHCO_3$ per 1 L of MilliQ water with pH adjusted to 7.3. Otherwise, Gt-coated sand was obtained in the same way as described above for biogenic Fh-coated sand except that inoculated serum bottles were kept in the dark at 30 °C.

Sand coated with a mix of lepidocrocite and goethite (Lep/Gt_1 an Lep/Gt_2) was prepared using Fe(III)-reducing cultures enriched from sediments collected at our study site in Van Phuc. The cultures were enriched from sediments collected at 30 m depth with a mix of acetate and lactate (5 mM each) as electron donor and 2-line ferrihydrite as electron acceptor under anoxic conditions. The Van Phuc artificial groundwater containing 0.01 g KH_2PO_4, 0.1 g NH_4Cl, 0.025 g $MgSO_4$ x 7 H_2O, 0.01 g $CaCl_2$ x 2 H_2O, 0.02 g $MnCl_2$, and 1.85 g $NaHCO_3$ per 1 L of MilliQ water with pH adjusted to 7.3 was used as a growth medium. The culture showed robust Fe(III)-reducing capacity (see Fig. S1) and *Geobacter* sp. was determined as a dominate taxon via denaturing gradient gel electrophoresis (DGGE) and sequencing of the most prominent bands. However, the two enrichment cultures had obviously a different microbial community composition and/or activity since obtained minerals, although both were identified as a mix of lepidocrocite and goethite, differed in color, Fe content, and As sorption capacity (see section 3.1 and 3.3). The abiogenic Fh-coated sand (produced as described above) and the Van Phuc artificial groundwater medium were inoculated with the enrichment culture and kept in horizontal position in the dark at 30 °C. Bottles were turned every day by hand until no change of color was observed anymore. The formed mixture of Lep/Gt was likely a result of secondary mineral formation during Fh reduction (Boland et al., 2014; Hansel et al., 2005).

Finally, a mix of biogenic lepidocrocite and magnetite (Lep/Mt) coated sand was prepared as previously described by Sorwat et al. (2020). The obtained mineral was not pure and consisted of a mixture of lepidocrocite and magnetite. The identity of the Fe minerals formed was determined by temperature dependent magnetic susceptibility.

Again, the geochemistry and mineralogy of the biogenic mineral coated sand grains was analyzed before and after the incubation experiment as described below.

2.4. In-situ Fe(III) mineral incubation

The synthesized biogenic and abiogenic Fe(III) minerals coated on sand were used for the in-situ exposure experiment. One part of the minerals (biogenic Fh, Gt, Lep/Mt, Lep/Gt_1, Lep/Gt_2 and abiogenic Fh, Gt, Mt and Hem) was placed in a wafer (a 3D printed frame covered from both sides with 0.2 mm nylon mesh membrane; Fig. 1A) as previously described in (Neidhardt et al., 2018). The second part of the minerals (biogenic Fh, Gt, Lep/Mt, Lep/Gt_1, abiogenic Fh, Gt, Hem and Mt and uncoated, HCl washed sand used as a control) was placed directly in pouches made from a permeable 0.2 mm nylon mesh membrane tightened with nylon cable ties (Fig. S2). Two identical sets of wafers and pouches containing 4.5 g of each mineral were prepared. Wafers and pouches were attached to 0.55 mm nylon fishing line, weighed down with stainless steel hex nuts and placed in the monitoring wells for a period of 3 weeks. One set was incubated in the strongly reducing As-contaminated, Fe^{2+}- and CH_4-rich well (25 m), while the other one in low As, Fe^{2+} and CH_4-free well (32 m) (Fig. 1B). Both wells are located within a few meters from each other (20°55′18.4″ 105°53′38.3″) and referred to AMS 11(25) and AMS 11(32) in our previous work

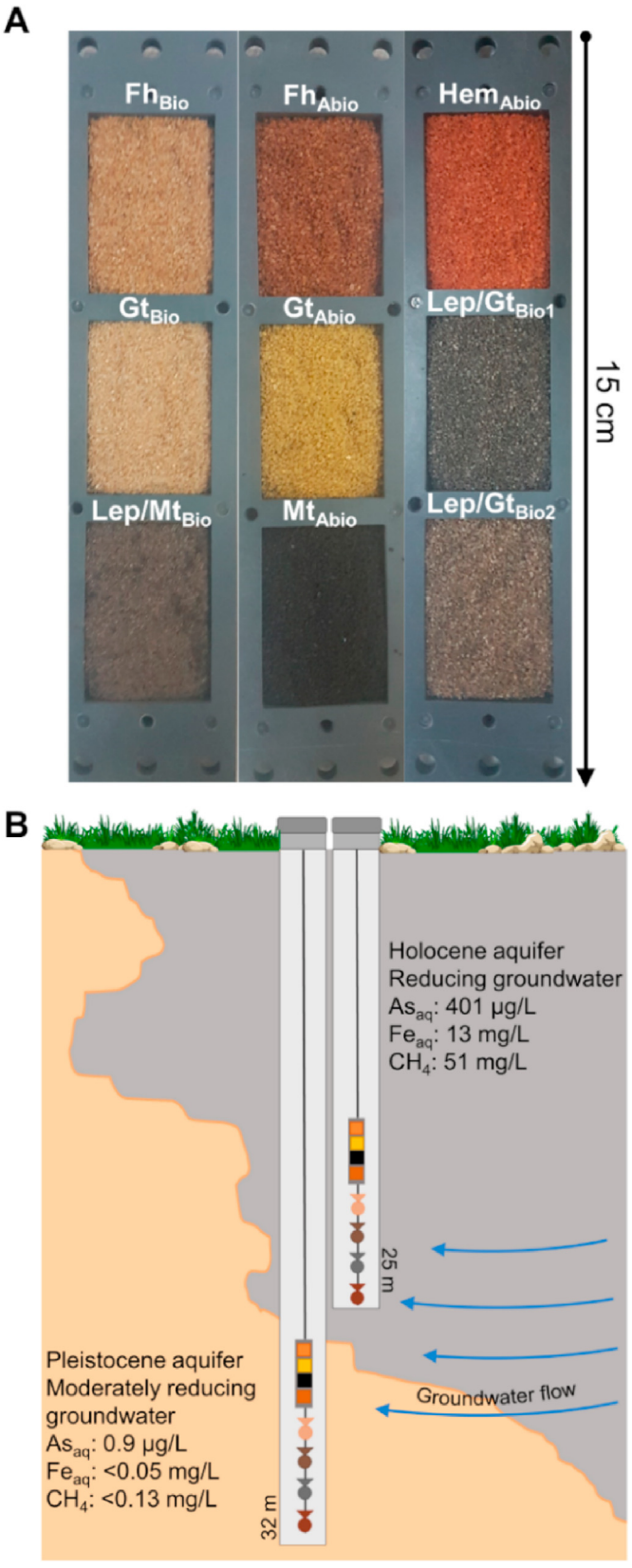

Fig. 1. The wafers containing different biogenic (Bio) and abiogenic (Abio) minerals used for incubation (A). Ferrihydrite (Fh), goethite (Gt), magnetite (Mt), hematite (Hem), mix of lepidocrocite and goethite (Lep/Gt), and mix of lepidocrocite and magnetite (Lep/Mt). Schematic cross-section of the As-contaminated strongly reducing and As-free moderately reducing aquifers with wells where wafers (▮) and mash bags (🐞) containing different minerals were incubated for 3 weeks (B).

(Glodowska et al., 2020c; Stopelli et al., 2020) where detailed information about groundwater hydrochemistry and microbiology can be found and is summarized in Table S1.

2.5. Sampling and sample preservation

After 3 weeks of incubation, the incubated wafers and pouches were recovered from the wells. The wafers were immediately placed in water- and air-tight zip-lock bags flushed with N_2 and kept on dry ice. Bags (PET/PE-LD/Aluminum stand-up pouches LamiZip, DAKLAPACK) with very low oxygen and water vapor permeability and protection against UV radiation were used to minimize sample alteration during transport and storage. The samples were analyzed for the solid-phase geochemistry and mineralogy.

Minerals incubated in the mesh pouches were immediately transferred to 15 mL sterile Falcon tubes and immersed in LifeGuard Soil Preservation Solution (Qiagen) to stabilize microbial DNA and RNA. Samples were stored on dry ice during transport, placed in a −80 °C freezer upon arrival at the laboratory and later used for 16S rRNA gene amplicon sequencing and qPCR analysis.

2.6. Geochemistry and mineralogy

Before analysis, the minerals were removed from the wafer in a glovebox and dried in a desiccator with drying granulate (Roth Silica gel orange 1–3 mm) under N_2 atmosphere (Air liquid UN 1066, ≥99,8 vol%) at 40 °C for 48h to avoid alteration of redox and temperature sensitive phases. Samples for geochemical analysis were grinded to a homogenous fine powder (<63 µm) using a ball mill before being analyzed. Fe and As concentrations of grounded sample material was analyzed using energy dispersive X-ray fluorescence (XRF) (Epsilon 5, PANalytical). The ED-XRF detection limit for As is 1 mg/kg.

Bulk mineral composition of reaction components was determined by XRD (Bruker D8 Discover) at the LERA (KIT). CuKα-radiation was used and the samples were scanned from 2° 2θ to 82° 2θ with an increment of 0,02° 2θ at 0.4 s. The relative mineral abundances were estimated from integrated peak areas using the HighScore-Plus software from Malvern Panalytical GmbH and the Inorganic Crystal Structure Database (ICSD) for phase identification. Temperature dependent magnetic susceptibility was determined on nitrogen flushed samples with a KLY-4S kappabridge (Agico) from −196 °C (liquid nitrogen temperature) to 710 °C for Fe mineral identification. High temperature measurements (room temperature to 710 °C) were measured in an inert argon atmosphere to minimize oxidation. The analyses were done in the structural geology division at KIT.

For microscopic analyses, the wafer samples were embedded directly into a synthetic resin (Araldite, 2020) to avoid any oxidation. The subsequent hardening process was conducted under vacuum to ensure in-depth impregnation and exclusion of oxygen. The temperature during the whole process was always below 40 °C to avoid any thermal alteration of the Fe phases.

The Scanning Electron Microscope (SEM-EDX) measurements were done using a Tescan Vega 2 SEM with an Oxford Instruments Silicon Drift Detector (SDD) INCAx-act for Energy Dispersive X-ray Spectroscopy (EDX) analysis for quantitative elemental analyses operating at an accelerating voltage of 15 kV, using the secondary electron (SE) and backscatter (BS) signal. Thin sections were mounted on specific 3D-printed sample holders and measured with carbon or gold coatings. Identification of elements in spot analyses and their distribution using the mapping option of automatic or manual search of elements were performed using the analytical software SwiftED (version 1.2). Element abundances

were determined from the EDS spectra by integrating peak areas and normalizing the results to 100%. Selected spots were analyzed with a FEI Quanta 650 FEG ESEM coupled to a Bruker QUANTAX, Esprit 1.9ED-XRF to obtain higher resolution. All analysis were done in the Laboratory for Environmental and Raw Material Analysis at KIT.

2.7. 16S rRNA gene amplicon sequencing and qPCR

DNA was extracted using a phenol-chloroform method following a protocol from Lueders et al. (2004). DNA was eluted in 50 μL of a 10 mM Tris buffer. DNA concentration was determined using a Qubit® 2.0 Fluorometer with DNA HS kits (Life Technologies, Carlsbad, CA, USA). Bacterial and archaeal 16S rRNA genes were amplified using universal primers 515f: GTGYCAGCMGCCGCGGTAA (Parada et al., 2016) and 806r: GGACTACNVGGGTWTCTAAT (Apprill et al., 2015) fused to Illumina adapters. The PCR cycling conditions were as follows: 95 °C for 3 min, 25 cycles of 95 °C for 30s, 55 °C for 30 s, and 75 °C for 30 s. These steps were followed by a final elongation step at 72 °C for 3 min. The quality and quantity of the purified amplicons were determined using agarose gel electrophoresis and NanoDrop (NanoDrop 1000, Thermo Scientific, Waltham, MA, USA). Subsequent library preparation steps and Illumina MiSeq sequencing (Illumina, San Diego, CA, USA) using the 2 × 250 bp MiSeq Reagent Kit v2 (500 cycles kit) were performed at Microsynth AG (Balgach, Switzerland). Between 86,887 and 187,365 read pairs were obtained for each sample.

Sequencing data was analyzed with nf-core/ampliseq v1.1.0, which includes all analysis steps and software and is publicly available (Ewels et al., 2020; Straub et al., 2020). Primers were trimmed, and untrimmed sequences were discarded (<3% per sample) with Cutadapt version 1.16 (Martin, 2011). Adapter and primer-free sequences were imported into QIIME2 version 2018.06 (Bolyen et al., 2019), their quality was checked with demux (https://github.com/qiime2/q2-demux), and they were processed with DADA2 version 1.6.0 (Callahan et al., 2016) to eliminate PhiX contamination, trim reads (before median quality drops below 35; forward reads were trimmed at 230 bp and reverse reads at 219 bp), correct errors, merge read pairs, and remove PCR chimeras; ultimately, in total 5741 amplicon sequencing variants (ASVs) were obtained across all samples. Alpha rarefaction curves were produced with the QIIME2 diversity alpha-rarefaction plugin, which indicated that the richness of the samples had been fully observed. A Naive Bayes classifier was fitted with 16S rRNA gene sequences extracted from the SILVA version 132 SSU Ref NR 99 database (Pruesse et al., 2007), using the PCR primer sequences. ASVs were classified by taxon using the fitted classifier (https://github.com/qiime2/q2-feature-classifier). ASVs classified as chloroplasts or mitochondria were removed. The number of removed ASVs was 21, totaling to <0.5% relative abundance per sample, and the remaining ASVs had their abundances extracted by feature table (Pruesse et al., 2007).

Raw sequencing data have been deposited at GenBank under BioProject accession number PRJNA686278 (https://www.ncbi.nlm.nih.gov/bioproject/PRJNA686278).

Quantitative PCRs specific for 16S rRNA genes of bacteria and archaea, methyl-coenzyme M reductase subunit alpha (*mcrA*) genes, particulate methane monooxygenase (*pmoA*) genes, and anaerobic arsenite oxidase (*arxA*) genes were performed. The qPCR primer sequences, gene-specific plasmid standards, and details on the thermal programs are given in Table S2. Quantitative PCRs on DNA extracts obtained as described above were performed in triplicate using SybrGreen® Supermix (Bio-Rad Laboratories GmbH, Munich, Germany) on the C1000 Touch thermal cycler (CFX96™ real time system). Each quantitative PCR assay was repeated three times, with triplicate measurements calculated for each sample per run. Data analysis was done using the Bio-Rad CFX Maestro 1.1 software version 4.1 (Bio-Rad, 2017).

3. Results and discussion

3.1. Fe(III) mineral dissolution in strongly reducing As-contaminated and moderately reducing As-free aquifer

The color of most Fe(III) mineral-coated sands (except for abiogenic Gt, Hem and Mt) used in our experiment became paler and even faded within 3 weeks of incubation. This implies that some of the Fe(III) minerals were transformed, dissolved by reductive dissolution or washed away with the groundwater flow. The geochemistry provided evidence for the loss of some Fe mineral coatings, especially in the Fh and Gt/Lep$_1$ samples (Fig. 2A).

We found that in the strongly reducing As-contaminated aquifer (25 m), in particular the abiogenic and biogenic Fh were reductively dissolved (loss of Fe_2O_3 from 1.6 g/kg sand to 0.5 g/kg and from 4.8 g/kg sand to 2.1 g/kg sand for the biogenic and abiogenic Fh, respectively, i.e., a loss of 67 and 56%) (Fig. 2A). In contrast, the more crystalline abiogenic Gt, Mt and Hem were not dissolved, indicated by the rather stable Fe_2O_3 content of ca. 1.9, 6.0 and 1.2 g/kg sand before and after incubation (Fig. 2A). Unlike the abiogenic crystalline minerals, we found that the biogenic crystalline minerals such as Gt and the mixture of Lep/Gt$_1$ also were reduced and dissolved as indicated by the change of Fe_2O_3 concentration from 0.8 to 0.5 g/kg for Gt and from 14 to 6 g/kg for Lep/Gt$_1$ after incubation (loss of 40% and 58% of Fe_2O_3, respectively). Yet, the Lep/Gt$_2$ behaved differently as its Fe_2O_3 content remained stable (1.7 g/kg) and it was not dissolved.

When incubating the minerals in the As-free moderately reducing aquifer (32 m), we observed that Fe_2O_3 concentration of poorly crystalline biogenic and abiogenic Fh decreased from 1.6 to 0.3 g/kg and from 4.7 to 3.1 g/kg, respectively, corresponding to a loss of 83% and 34% of Fe_2O_3 (Fig. 2A). While more crystalline abiogenic Fe minerals such as Gt, Mt and Hem remained rather stable, biogenic Gt, Lep/Gt$_1$, Lep/Gt$_2$ and Lep/Mt appeared to be less stable as indicated by a decrease in the Fe_2O_3 content of 56, 47, 4 and 11%, respectively (Fig. 2A).

Our observations are supported by previous studies by Zachara et al. (2002) who found that poorly crystalline Fe(III) phases such as Fh were unstable under reducing and oxidizing conditions. Further studies have shown that biominerals are more easily reduced by microorganisms due to their lower crystallinity, smaller particle size (larger surface area) and the content of organic molecules (Langley et al., 2009; Roden, 2004). Hence, biogenic (and abiogenic) Fe minerals were reduced to certain extent via microbially mediated Fe(III) reductive dissolution within 3 weeks of incubation. It should be kept in mind however, that biogenic minerals tend to incorporate and coprecipitate more elements (Al, Ca, Si, P) in the crystal lattice (Fortin and Langley, 2005; Kiskira et al., 2019; Voegelin et al., 2010) than abiotic Fe minerals. These incorporations weaken the crystal structure facilitating its dissolution. Besides, biogenic Fe minerals such as Mt tend to have smaller grain sizes than the abiotic counterparts (Karlin, 1990) and a poorly crystalline-microcrystalline structure which may increase dissolution of these minerals. Finally, biogenic minerals tend to incorporate organic substances e.g., bacterial cells (Ferris, 2005) and often form organo-mineral complexes which can also be dissolved more easily. Therefore, biogenic minerals are not only preferentially exploited by microorganisms but are also generally less stable than abiotically formed Fe minerals which may contribute to more pronounced loss of Fe in biogenic minerals in our experiment.

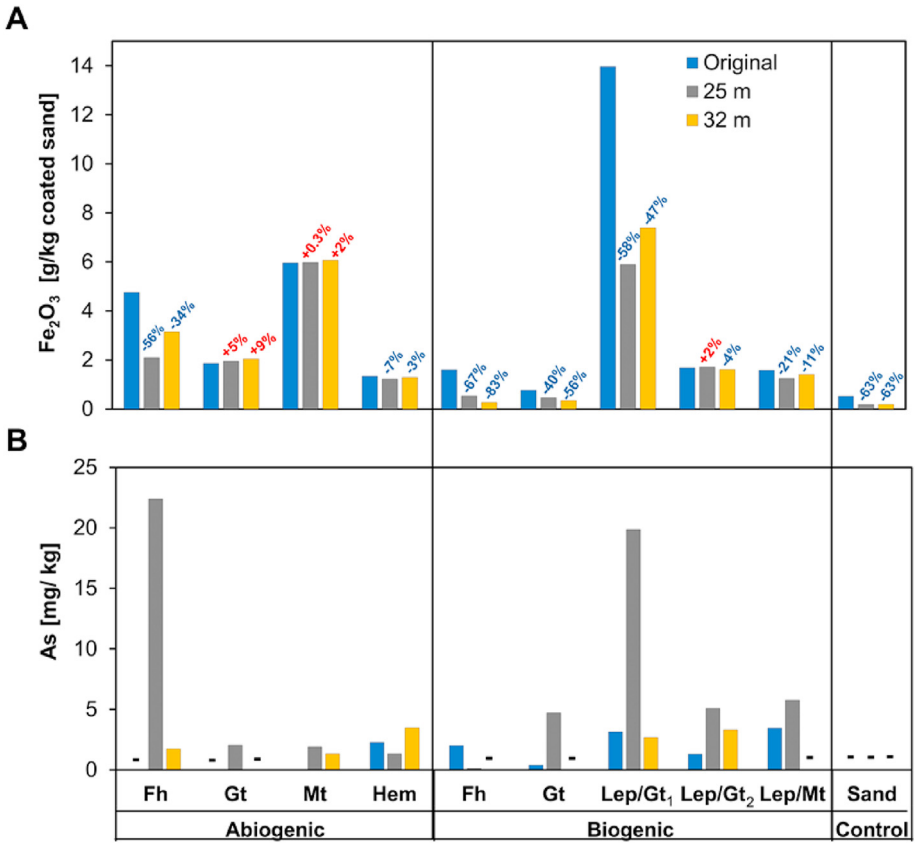

Fig. 2. Changes in Fe (A) and As content (B) in Fe mineral-coated sand after 3 weeks of incubation in As-contaminated strongly reducing water at 25m depth (gray) and As-free moderately reducing water at 32 m depth (yellow) compared to original minerals before incubation (blue). Ferrihydrite (Fh), goethite (Gt), magnetite (Mt), hematite (Hem), mix of lepidocrocite and goethite (Lep/Gt), and mix of lepidocrocite and magnetite (Lep/Mt), and uncoated sand used as a control. The % values indicate the loss or gain in Fe content relative to the initial one before incubation. (For interpretation of the references to color in this figure legend, the reader is referred to the Web version of this article.)

Although in the uncontaminated aquifer the conditions were less reducing based on redox potential (Table S1), substantial amounts of Fe were also mobilized, probably also by microbially mediated reductive dissolution. It appears that the uncoated control sand contained some initial coating with a small amount of Fe_2O_3 (<0.05 wt%) which got dissolved in both highly and moderately reducing conditions.

Intensive dissolution of Fe(III) minerals was further confirmed by SEM which revealed that Fe(III) mineral coatings resisted dissolution mainly in protected areas such as cavities between closely spaced sand grains (Fig. 3). The rough surfaces of the sand grains are not uniformly coated by the Fe(III) mineral, either indicating an incomplete original coating of the surface or dissolution. SEM-EDX spectra of all coatings confirm Fe and O as major elements and occasionally Si and Al were detected in minor amounts. Quartz grains coated by abiogenic Fh from the strongly reducing groundwater (25 m) often show intergrowth of two phases (Fig. 3A), with a brighter granular phase (Mt) and a gray surrounding phase (Fh). A two-phase intergrowth is also observed for the biogenic Fh in the moderately reducing groundwater, but distinctly less obvious (Fig. 3B). The biogenic Lep/Gt is characterized by needle-shaped to flaky grain shapes and do not show any transformation (Fig. 3C). Arsenic was not detected using SEM-EDX due to the high detection limit.

3.2. Fe(III) mineral transformation

Dissolution and transformation are widespread processes observed in the Fe(III) minerals exposed to As-contaminated strongly reducing as well as As-free less reducing groundwater (Figs. 2 and 3). Because of the low concentration of Fe, we were not able to identify the Fe minerals of the coatings using XRD analysis, and SEM-EDX provided information about elemental composition in the minerals only qualitatively. Therefore, we used temperature dependent magnetic susceptibility in the temperature range from −190° − 700 °C to identify the Fe mineralogy and transformation products (Fig. 4). These measurements showed that Mt is often present in the analyzed samples. Magnetite is a ferrimagnetic mineral that was identified based on the characteristic Verwey transition (T_V) at about −150 °C and its Curie temperature (T_C) at about 580 °C. The T_V is mostly very weak or even absent, which is indicative of very small grain size of secondary Mt (original grain size was 0.3 μm) or a significant vacancy concentration in the crystal lattice (Dunlop and Özdemir, 2007). During the 3 weeks exposure of Mt in strongly reducing As-rich and less reducing As-free groundwater, no significant changes occurred except that the T_V completely disappeared and T_C slightly increased. The relatively good reversibility of heating and cooling curve and the Hopkinson peak just before reaching T_C indicates pseudo-single domain grain sizes of magnetite <10 μm (Dunlop et al., 2007). The abiogenic Hem-coated sample shows already little Mt in the original sample. The higher magnetic susceptibility in the cooling curve indicates that Hem has transformed into Mt during the high-temperature measurement in argon atmosphere. In strongly reducing groundwater (25 m), only Mt remained indicating that Hem is either dissolved or transformed into Mt. In moderately reducing

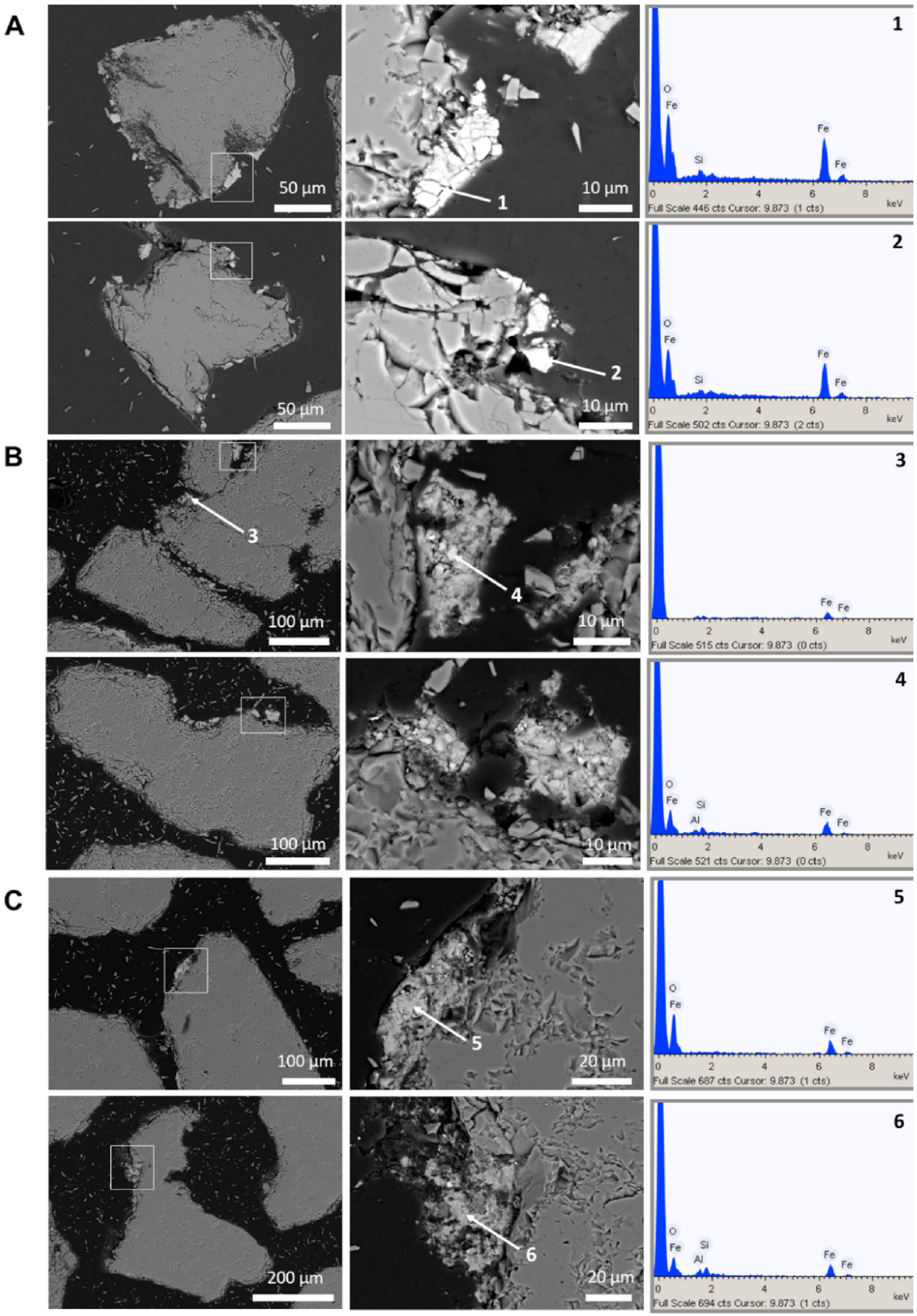

Fig. 3. Scanning electron micrographs (backscattering detector) of selected areas of (A) abiogenic Fh-coated sand incubated in the strongly reducing As-contaminated groundwater, (B) abiogenic Fh-coated sand incubated in the moderately reducing As-free groundwater, and (C) biogenic Lep/Gt_1-coated sand incubated in the strongly reducing As-contaminated groundwater. White squares indicate the analyzed area (zoomed in on the right side). In the right column, the EDX spectra for indicated position (white arrow) is presented.

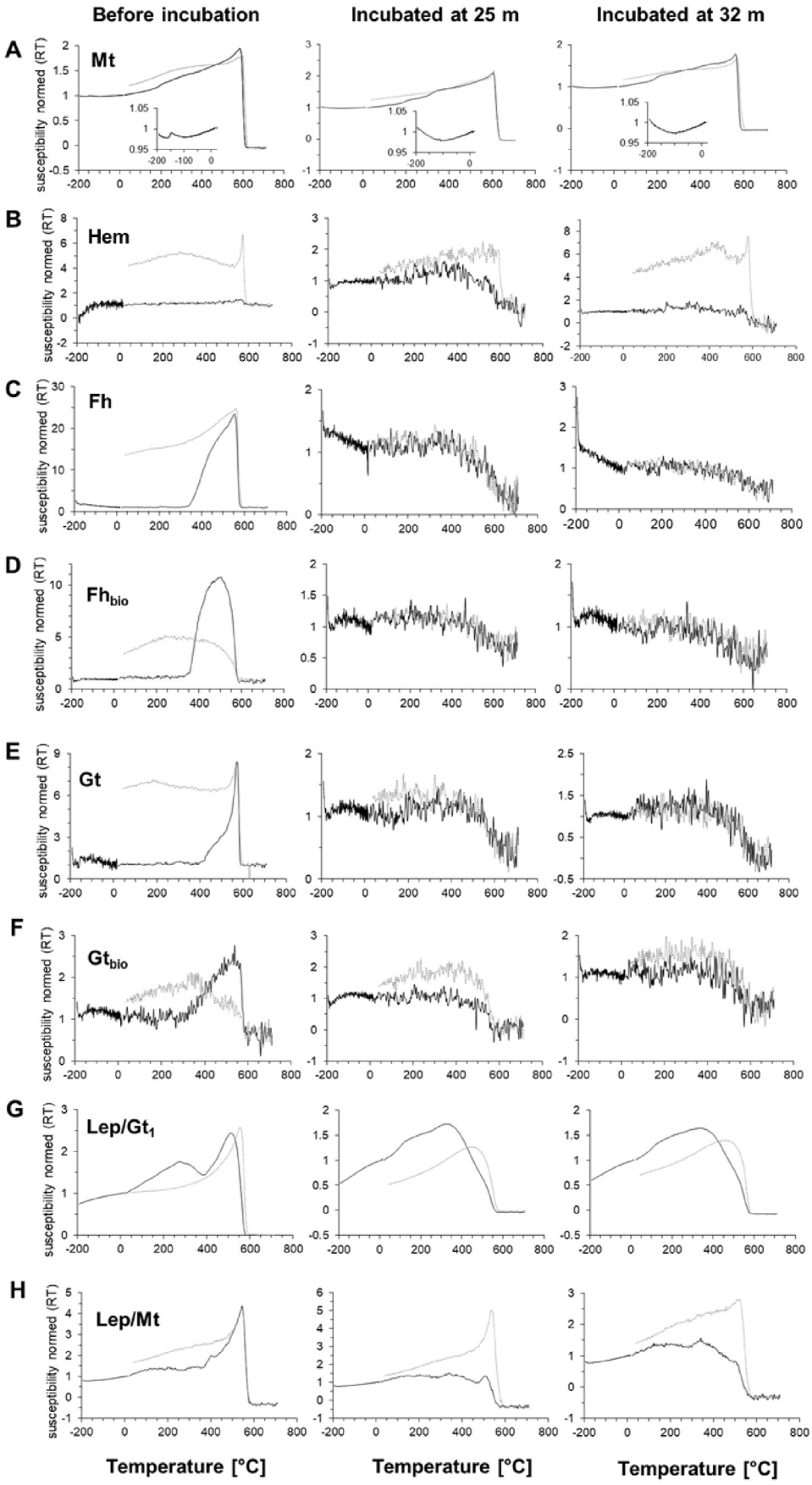

Fig. 4. Temperature depended magnetic susceptibility of (A) abiogenic Mt, (B) abiogenic Hem, (C) abiogenic Fh, (D) biogenic Fh, (E) abiogenic Gt, (F) biogenic Gt, (G) biogenic mix of Lep/Gt_1 and (H) biogenic mix of Lep/Mt before and after incubation in strongly reducing As-contaminated (25 m) and As-free moderately reducing groundwater (32 m). In black: heating curve, gray: cooling curve.

groundwater (32 m), no change occurred for Hem (Fig. 4B).

Although for the Gt and Fh samples very little Mt in the original sample cannot be excluded, they are characterized by Mt formation in both, strongly and moderately reducing groundwater (25 and 32 m) exposure. This seems to be more obvious in the abiogenic samples of the reduced environment than in the biogenic samples (Fig. 4C–F). Especially in the Fh samples and in the biogenic Gt the transformation into Mt is accompanied by strong dissolution (Fig. 2).

The two biogenic Lep/Gt samples strongly differ in their dissolution behavior (Fig. 2) but they both do not show major transitions, neither in strongly (25 m) nor moderately reducing groundwater (32 m) (Fig. 4G) suggesting that the biogenic mixed phases are relatively stable under both of these conditions. This is also the case for biogenic Lep/Mt although grain size changes in Mt seem to occur, indicated by the disappearance of the Hopkinson peak in the heating curves of the groundwater exposed samples (Fig. 4H).

In summary, all samples are characterized by dissolution and/or transformation processes. The most interesting observation is the transformation of biogenic and abiogenic Fh and Gt into Mt under both redox conditions and stability of that mixed biogenic Lep/Gt and Lep/Mt which are less susceptible for Fe-mineral transformations in these environments (Fig. 5).

3.3. As sorption to Fe minerals

The As concentration in most Fe(III) minerals, incubated in the strongly reducing water (25 m), is much higher compared to the Fe(III) minerals that were in contact with As-free moderately reducing water at 32 m depth (Fig. 2B) which is in agreement with the previous work at the same site (van Geen et al., 2013). This can mainly be explained by the higher dissolved As concentration in groundwater at 25 m depth. Clearly differences in the As content between the individual Fe(III) minerals (Fig. 2B), however, must be related to mineral specific characteristics and transformation processes. The point of zero charge is in a similar range (pH 7.0–7.6) for all investigated Fe(III) minerals (Borggaard, 1983; Rajput et al., 2016) and thus, a slightly positive to neutral surface charge is expectable at the local groundwater pH of ~7.1. This however, would equally favour the adsorption of As(V), as negatively charged oxyanion, to all minerals and could not explain the obvious differences in sorption affinity. The abiogenic Fh-coatings showed by far the highest sorption capacity towards As (22 mg As/kg), likely related to its specific surface area which is generally much larger compared to the other abiogenic Fe(III) minerals that were investigated (Borggaard, 1983; Rajput et al., 2016). Furthermore (Qi and Pichler, 2014), have shown that As(III), which is likely the dominant As species at the redox conditions in the groundwater, clearly outcompetes As(V) adsorption onto Fh above pH 6. Still, the very high As concentration of Fh in the strongly reducing groundwater at 25 m depth is somehow surprising due to the strong dissolution indicated by decreasing Fe content (Fig. 2A). Incorporation and fixation of As during mineral transformation could be one explanation (Fig. 5).

On the contrary, biogenic Fh did not sorb any detectable As. Biogenic, poorly crystalline Fe(III) minerals are also known to have a large specific surface area. However, they have a negative surface charge at a neutral pH due to the presence of biomass-derived organics (Posth et al., 2010). This strongly lowers the affinity regarding binding of As oxyanions. In fact, a previous study from our lab showed repulsion of negatively charged As(V) by the negatively charged biogenic Fe(III) (oxyhydr)oxides (Kleinert et al., 2011). Since water pH under both redox conditions is near neutral (7.1 and 7.4) low As affinity toward biogenic Fh due to negative surface charge may be a valid explanation. Additionally to the change in surface charge by cell-derived organic matter (CDOM) (Muehe et al., 2013b; Posth et al., 2010), the organic molecules and other impurities further decrease the sorption capacity by competitive sorption. Several studies demonstrated that presence of organic matter generally decrease sorption of As onto Fh (Grafe

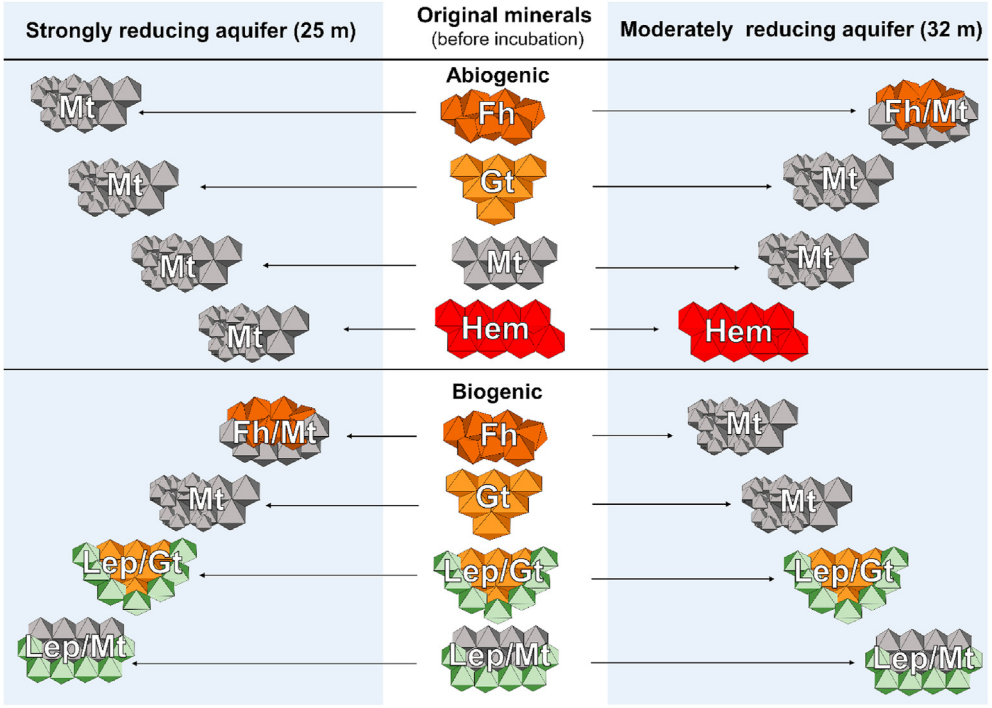

Fig. 5. Original Fe(III) minerals and their transformation products after 3 weeks of incubation in the Holocene (25 m) and Pleistocene aquifer (32 m). Ferrihydrite (Fh), goethite (Gt), magnetite (Mt), hematite (Hem), mix of lepidocrocite and goethite (Lep/Gt), and mix of lepidocrocite and magnetite (Lep/Mt).

et al., 2002) and Gt (Grafe et al., 2001).

Surprisingly, the mixed Lep/Gt$_1$ minerals biosynthesized by microbes from Van Phuc sediments sorbed remarkably high and compared to abiogenic Fh a similar amount of As (20 mg As/kg). This may be related to a different biomineralization pathway compared to biogenic Fh. The biogenic Fh was produced as an effect of microbially mediated precipitation of dissolved Fe^{2+}. Previous studies showed that Fe(III) by-products of this reaction, precipitate rapidly in the direct vicinity of the cells, leading to its encrustation (Miot et al., 2009; Schädler et al., 2009). Therefore, it is very likely that biomass incorporated within biogenic Fh prevents As sorption. On the contrary, the mixed phase of Lep/Gt was produced as an effect of Fe(III) reduction and secondary mineral precipitation, thus much less biomass is expected to be incorporated into the freshly formed mineral. Consequently, this type of mineral is suggested to sorb As more efficiently.

All the other biogenic Fe(III) minerals sorbed ~5 mg As/kg, while the abiogenic ones (except Fh) sorbed ~2 mg As/kg in the reducing aquifer. Overall, it can be observed that biogenic Fe(III) minerals (except Fh) are subjected to much more pronounced dissolution under strongly and moderately reducing conditions, However, they tend to sorb more As compared to abiogenic Fe(III) minerals.

3.4. Role of microbial processes in Fe(III) mineral transformation

In order to evaluate the potential involvement of microbial processes in Fe(III) mineral transformation and reduction, the microbial community structure and abundance was analyzed in all samples after 3 weeks of exposure (Figs. 6 and 7). Although, groundwater hydrochemistry significantly differed between the As-contaminated (25 m) and As-free aquifer (32 m), the microbial community composition from exposed minerals showed certain similarities.

3.4.1. Microbial Fe(III) reduction and its influence on mineral transformation

Putative Fe(III)-reducing bacteria appeared to be the most abundant group of microorganisms colonizing Fe(III) minerals under both redox-conditions (Fig. 6). Among known Fe(III)-reducers, taxa related to *Geobacter* showed the highest relative abundance in most samples. *Geobacter* spp. are well-known Fe(III) reducers, previously shown to be capable of reducing As-bearing Fe(III) minerals and to contribute to As mobilization (Glodowska et al., 2020a; Islam et al., 2005a, 2005b). These bacteria, besides using Fe(III) as electron acceptor, may also reduce As(V) while oxidizing organic carbon (Héry et al., 2008). Despite its high abundance among all samples, taxa affiliating with *Geobacter* were mainly thriving on abiogenic Fh, where they represented 31% and 27% of total 16S rRNA gene sequences in strongly reducing As-contaminated (25 m) and less reducing As-free (32 m) groundwater incubated samples, respectively (Fig. 6). Poorly crystalline Fh provide the more bioavailable form of Fe(III) that is preferentially exploited by Fe(III)-reducing microorganisms as a terminal electron acceptor (Lovley et al., 1991). Moreover, it was previously shown in batch experiments that Fh is often fully reduced or transformed to secondary Fe(II)-containing minerals (Fredrickson et al., 1998a,

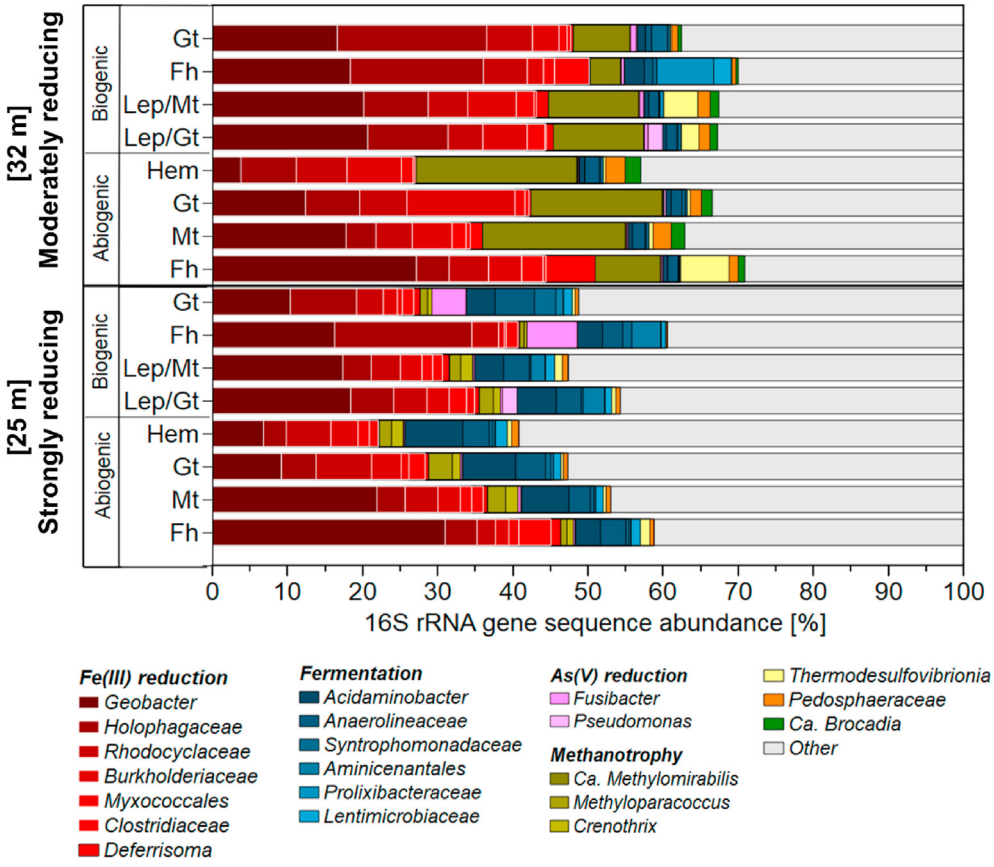

Fig. 6. Composition and putative function of microbial communities associated with different abiogenic and biogenic Fe(III) minerals, incubated for 3 weeks in an As-contaminated strongly reducing and in an As-free moderately reducing aquifer. Ferrihydrite (Fh), goethite (Gt), magnetite (Mt), hematite (Hem), mix of lepidocrocite and goethite (Lep/Gt), and mix of lepidocrocite and magnetite (Lep/Mt).

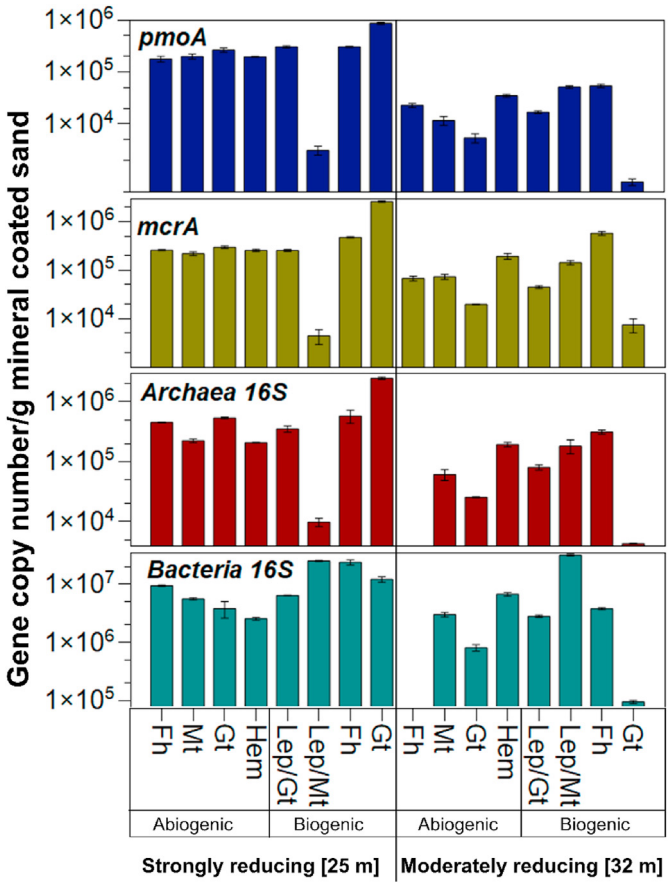

Fig. 7. Bacterial and archaeal 16S rRNA gene, *pmoA* and *mcrA* copy numbers per 1 g mineral coated sand in biomass associated with abiogenic and biogenic Fe(III) minerals that were incubated for 3 weeks in an As-contaminated strongly reducing and an As-free moderately reducing aquifer. Ferrihydrite (Fh), goethite (Gt), magnetite (Mt), hematite (Hem), mix of lepidocrocite and goethite (Lep/Gt), and mix of lepidocrocite and magnetite (Lep/Mt).

2001), while Gt and Hem are only partially reduced (Zachara et al., 1998). This might explain more advanced dissolution of biogenic and abiogenic Fh in both environments, compared to Hem and Gt. Furthermore, in our experiment, the more crystalline minerals such as Hem and Gt revealed substantially lower relative abundance of *Geobacter* and other Fe(III) reducers (3–16%), suggesting a generally lower bioavailability of these minerals. The *Holophagaceae* family was the second most abundant taxon found on incubated Fe(III) minerals, however, many sequences within this family remained unassigned. Further analysis of these unassigned sequences using BLAST revealed that most of the *Holophagaceae* taxa were closely related to *Geothrix fermentans*, another well-known Fe(III) reducer (Coates et al., 1999; Islam et al., 2005a), which was probably involved in magnetite formation, as previously demonstrated (Klueglein et al., 2013). Taxa affiliating with *Rhodocyclaceae*, *Burkholderiaceae*, *Myxococcales*, *Clostridiaceae* and *Deferrisoma* that were previously shown or suggested to be involved in Fe(III) reduction (Li and Peng, 2011; Pérez-Rodríguez et al., 2016; Slobodkina et al., 2012; Treude et al., 2003; Zhang et al., 2020), were also abundant among all analyzed mineral samples. Overall, it appears that the relative abundance of Fe(III)-reducing taxa was higher in biogenic minerals incubated in the moderately reducing (32 m) rather than in those incubated in strongly reducing groundwater (25 m). Yet, bacterial and archaeal 16S rRNA gene copy number was higher in Fe(III) minerals retrieved from As-contaminated aquifer (25 m), implying that generally more microorganisms thrive in As-, Fe- and CH_4-rich water (Fig. 7). Besides abiogenic Fh that hosted the highest relative abundance of Fe(III) reducers, it can be noticed that biogenic Fe(III) minerals tended to host more bacteria and archaea (Fig. 7) and showed higher relative abundance of putative Fe(III)-reducers compared to abiogenic minerals (Fig. 6). This indicates that biogenic Fe(III) minerals will likely get reduced or transformed by dissimilatory metal-reducing bacteria faster than abiogenic minerals and might explain why biogenic minerals were generally more dissolved compared to abiogenic ones.

The end product of the microbially mediated Fe(III) reduction depends on several factors. Besides the identity of primary minerals, the identity of secondary minerals depends on the medium composition, concentration of electron donor and acceptor, Fe(III) mineral age, sorbed ions, co-associated Fe(III) oxides (Zachara et al., 2002) and likely on the abundance and the composition of the microbial community mediating the reaction. Therefore, it is very difficult to predict what kind of secondary minerals might be produced under natural conditions. It was however shown that Fh, if not completely reduced, is often transformed into secondary Fe(II)-containing minerals, such as siderite (in buffered medium), magnetite or green rust (Fredrickson et al., 1998b; Muehe et al., 2013a, 2013b). More crystalline minerals such as Gt and Hem tend to remain largely unchanged or get partially converted to vivianite, magnetite or green rust (Cutting et al., 2009; Muehe et al., 2013b; Zachara et al., 1998). This is in agreement with our results (Fig. 5) which showed almost complete dissolution of Fh or its partial transformation to Mt (mainly under strongly reducing condition) and only fractional transformation of Gt and Hem.

3.4.2. The putative role of fermenters in Fe(III) reduction

Based on 16S rRNA gene sequencing (Fig. 6), it appears that typical fermenters belonging to *Firmicutes* (*Acidaminobacter*, *Syntrophomonadaceae*), *Bacteroidetes* (*Lentimicrobiaceae*, *Prolixibacteraceae*), *Chloroflexi* (*Anaerolineaceae*) and *Acidobacteria* (*Aminicenantales*) (Gupta et al., 2014; Kampmann et al., 2012; Tan et al., 2015; Wang et al., 2020) were abundant among exposed minerals. These fermenters were particularly abundant on minerals incubated in the strongly reducing shallow aquifer (25 m) where they accounted for 8–14% of the microbial community. This is likely related to the fact, that groundwater at this depth had 4 times more dissolved organic carbon (DOC) compared to the deeper moderately reducing aquifer (Table S1). Previous studies already indicated that many fermenters can use Fe(III) as electron acceptor (Dong et al., 2017; Esther et al., 2015; Zhao et al., 2020). Therefore, we hypothesize that fermenters abundantly found in Fe(III) minerals incubated in the As-contaminated strongly reducing aquifer (25 m) were in fact exploiting Fe(III) minerals as electron acceptors and subsequently contributed to Fe(III) reduction while oxidizing DOC. The relative abundance of putative fermenters appeared to be similar in biogenic and abiogenic minerals incubated in the As-contaminated aquifer (25 m). On the contrary, only biogenic Fh and to a lower extent biogenic Gt, incubated in the As-free environment (32 m), revealed a higher relative abundance of fermenters, which represented 14% and 4% of the microbial community, respectively. Our previous study investigating microbial communities across both aquifers in Van Phuc revealed that fermenters were indeed a dominant microbial group in groundwater (Glodowska et al., 2020c). Despite their dominance among exposed minerals, Fe(III) reducers, although present in most of the wells, represented only a small fraction (up to 2%) of the groundwater microbial community. This implies that Fe(III) reducers require physical contact with minerals in order to use Fe(III) as electron acceptor, while fermenters may use a wide range of electron

acceptors present in the water.

3.4.3. Involvement of methanotrophs in Fe(III) reduction and transformation

Methanotrophs are another microbial group enriched on the exposed minerals (Fig. 6). Interestingly, these microorganisms were highly abundant on minerals incubated in the lower As-free aquifer (32 m) where CH_4 is undetectable, while they were much less abundant in the strongly reducing upper aquifer (25 m) which is characterized by a very high CH_4 concentration (51 mg/L; Table S1). We have observed this phenomenon also in our previous study in Van Phuc, where methanotrophs appeared to be much more abundant in the CH_4-free groundwater compared to groundwater rich in CH_4 (Glodowska et al., 2020c) and in the deeper sediments associated with CH_4-free groundwater compared to shallow sediments where CH_4-rich groundwater is present (Glodowska et al., 2021). We hypothesize that this might be due to 1) intensive methanotrophy that led to depletion of CH_4 in the deeper part of the aquifer and to significant biomass production or 2) shortage of electron acceptors in the strongly reduced aquifer. Either way, methanotrophs were apparently attracted to Fe(III) minerals exposed to uncontaminated moderately reducing water (32 m) as they represented between 4 and 21% of the microbial community. On the contrary, methanotrophs represented only 1–4% of 16S rRNA gene sequences in the minerals incubated in the strongly reducing groundwater (25 m). Several previous studies have demonstrated that anaerobic CH_4 oxidation can be coupled to Fe(III) reduction (Aromokeye et al., 2020; Cai et al., 2018; Ettwig et al., 2016). Moreover, our earlier study confirmed that this process indeed takes place in Van Phuc and contributes to As mobilization (Glodowska et al., 2020b). However, in all of the previous studies archaea belonging to *Methanosarcinales* were shown to catalyze this process and to date there was no report of bacteria capable of mediating this reaction. Yet, the methanotrophic community thriving on the Fe(III) minerals in our experiment was generally dominated by bacteria related to *Candidatus* Methylomirabilis, *Methyloparacoccus* and *Crenothrix*. Abiogenic crystalline Fe(III) minerals such as Hem, Mt and Gt, incubated in less reducing groundwater (32 m) appeared to be preferentially associated with Ca. *Methylomirabilis* which represented 21, 19 and 17% of the microbial community, respectively. Although we previously found this taxon mainly in the moderately reducing As-free environment, its abundance was never that high, neither in the groundwater (max. 8%) nor in the sediments (max. 5%) (Glodowska et al., 2020b; Glodowska et al., 2021). A previous study already suggested that Ca. *Methylomirabilis* can use Fe(III) instead of NO_2^- as electron acceptor (Shen et al., 2019). Therefore it can be hypothesized that bacteria belonging to Ca. *Methylomirabilis* can use Fe(III) as electron acceptor either alone or in syntropic collaboration with other community members. The Fe(III) minerals exposed to As-contaminated strongly reducing groundwater (25 m) were much less associated with methanotrophs and taxa related to *Methyloparacoccus* and *Crenothrix* being most abundant. Here, also abiogenic more crystalline minerals such as Mt and Gt were preferentially colonized. The high abundance of *pmoA* and *mcrA* genes among the microbial community associated with Fe(III) minerals further highlight the involvement of methanotrophs in Fe(III) reduction and transformation (Fig. 7).

4. Conclusions

Biogenic Fe(III) minerals have different properties compared to their abiogenic counterpart and, in consequence, they behave differently in the natural environment. Our study indicates that biogenic minerals are preferentially occupied by bacteria and host higher relative abundances of Fe(III) reducers. As a result, this type of Fe(III) minerals are more prone to transformation and reduction even under moderately reducing conditions. *Geobacter* and *Holophagaceae* taxa are probably key players in Fe(III) reduction in both aquifers. Furthermore, the results of our exposure experiment implies involvement of fermenters and methanotrophs in Fe(III) reduction.

The environmental conditions are important factors influencing the behavior of Fe(III) minerals and their stability. At the investigated field site we observed a strong reductive dissolution of biogenic Fe(III) minerals or their transformation into Mt. On the other hand, biogenic minerals (except for Fh) tend to sorb more As. If As is sorbed/incorporated into Mt, into further secondary transformation products or into the original Fe(III) minerals has to be investigated in future by μ-XANES studies. Biominerals such as Lep/Gt biosynthesized using native microbial communities from Van Phuc were less prone to reduction and transformation and showed much higher affinity towards As, suggesting that this type of minerals might be more representative for this specific environment. It also implies that As and Fe dynamic in Van Phuc is largely controlled by indigenous microbial community.

Moreover, we believe that using a set of different Fe(III) minerals as a decoy may be an efficient strategy to assess the Fe(III) reducing capacity of the native microbial community and to capture the key Fe(III) reducers for further study and isolation.

Credit author statement

Martyna Glodowska: Conceptualization, Methodology, Investigation, Writing – original draft, Writing – review & editing, Visualization. Magnus Schneider: Conceptualization, Methodology, Writing – review & editing, Investigation, Visualization. Elisabeth Eiche: Writing – review & editing, Formal analysis. Agnes Kontny: Writing – review & editing, Formal analysis. Thomas Neumann: Supervision, Funding acquisition, Project administration. Daniel Straub: Data curation, Formal analysis, Software. Sara Kleindienst: Writing – review & editing, Funding acquisition, Resources. Andreas Kappler: Supervision, Writing – review & editing, Funding acquisition, Resources

Declaration of competing interest

The authors declare that they have no known competing financial interests or personal relationships that could have appeared to influence the work reported in this paper.

Acknowledgments

The authors thank all AdvectAs project members for the collaboration and support. Special thanks to Pham Hung Viet, Pham Thi Kim Trang, Vi Mai Lan, Mai Tran and Viet Nga from Hanoi University of Science for the assistance during the sampling campaign. This study was supported by the Deutsche Forschungsgemeinschaft (DFG) (KA 1736/41–1). D. Straub is funded by the Institutional Strategy of the University of Tübingen (DFG, ZUK 63) and by the Collaborative Research Center CAMPOS (Grant Agreement SFB 1253/1 2017). S. Kleindienst is funded by an Emmy-Noether fellowship (DFG, grant #326028733). The authors acknowledge support by the High Performance and Cloud Computing Group at the Zentrum für Datenverarbeitung of the University of Tübingen, the state of Baden-Württemberg through bwHPC and the German Research Foundation (DFG) through grant no INST 37/935-1 FUGG.

Appendix A. Supplementary data

Supplementary data to this article can be found online at https://doi.org/10.1016/j.envpol.2021.117012.

References

Abramov, S.M., Tejada, J., Grimm, L., Schädler, F., Bulaev, A., Tomaszewski, E.J., Byrne, J.M., Straub, D., Thorwarth, H., Amils, R., Kleindienst, S., Kappler, A., 2020. Role of biogenic Fe(III) minerals as a sink and carrier of heavy metals in the Rio Tinto, Spain. Sci. Total Environ. 718, 137294. https://doi.org/10.1016/j.scitotenv.2020.137294.

Apprill, A., McNally, S., Parsons, R., Weber, L., 2015. Minor revision to V4 region SSU rRNA 806R gene primer greatly increases detection of SAR11 bacterioplankton. Aquat. Microb. Ecol. 75, 129–137. https://doi.org/10.3354/ame01753.

Arain, M.B., Kazi, T.G., Baig, J.A., Jamali, M.K., Afridi, H.I., Shah, A.Q., Jalbani, N., Sarfraz, R.A., 2009. Determination of arsenic levels in lake water, sediment, and foodstuff from selected area of Sindh, Pakistan: estimation of daily dietary intake. Food Chem. Toxicol. 47, 242–248. https://doi.org/10.1016/j.fct.2008.11.009.

Aromokeye, D.A., Kulkarni, A.C., Elvert, M., Wegener, G., Henkel, S., Coffinet, S., Eickhorst, T., Oni, O.E., Richter-Heitmann, T., Schnakenberg, A., Taubner, H., Wunder, L., Yin, X., Zhu, Q., Hinrichs, K.-U., Kasten, S., Friedrich, M.W., 2020. Rates and microbial players of iron-driven anaerobic oxidation of methane in methanic marine sediments. Front. Microbiol. 10 https://doi.org/10.3389/fmicb.2019.03041.

Bakatula, E.N., Molaudzi, R., Nekhunguni, P., Tutu, H., 2016. The removal of arsenic and uranium from aqueous solutions by sorption onto iron oxide-coated zeolite (IOCZ). Water. Air. Soil Pollut 1, 1–14. https://doi.org/10.1007/s11270-016-3190-7.

Berg, M., Trang, P.T.K., Stengel, C., Buschmann, J., Viet, P.H., Van Dan, N., Giger, W., Stüben, D., 2008. Hydrological and sedimentary controls leading to arsenic contamination of groundwater in the Hanoi area, Vietnam: the impact of iron-arsenic ratios, peat, river bank deposits, and excessive groundwater abstraction. Chem. Geol. 249, 91–112. https://doi.org/10.1016/j.chemgeo.2007.12.007.

BGS and DPHE, 2001. Arsenic contamination of groundwater in Bangladesh. In: Kinniburgh, D.G., Smedley, P.L. (Eds.), British Geological Survey Technical Report WC/00/19. British Geological Survey, Keyworth.

Boland, D.D., Collins, R.N., Miller, C.J., Glover, C.J., Waite, T.D., 2014. Effect of solution and solid-phase conditions on the Fe(II)-Accelerated transformation of ferrihydrite to lepidocrocite and goethite. Environ. Sci. Technol. 48, 5477–5485. https://doi.org/10.1021/es4043275.

Bolyen, E., Rideout, J.R., Dillon, M.R., Bokulich, N.A., Abnet, C.C., Al-Ghalith, G.A., Alexander, H., Alm, E.J., Arumugam, M., Asnicar, F., Bai, Y., 2019. Reproducible, interactive, scalable and extensible microbiome data science using QIIME 2. Nature biotechnology 37 (8), 852–857.

Borggaard, O.K., 1983. Effect of surface area and mineralogy of iron oxides on their surface charge and anion-adsorption properties. Clay Clay Miner. 31, 230–232. https://doi.org/10.1346/CCMN.1983.0310309.

Cai, C., Leu, A.O., Xie, G.-J., Guo, J., Feng, Y., Zhao, J.-X., Tyson, G.W., Yuan, Z., Hu, S., 2018. A methanotrophic archaeon couples anaerobic oxidation of methane to Fe(III) reduction. ISME J. 12, 1929–1939. https://doi.org/10.1038/s41396-018-0109-x.

Callahan, B.J., McMurdie, P.J., Rosen, M.J., Han, A.W., Johnson, A.J.A., Holmes, S.P., 2016. DADA2: high-resolution sample inference from Illumina amplicon data. Nat. Methods 13, 581–583. https://doi.org/10.1038/nmeth.3869.

Chatain, V., Bayard, R., Sanchez, F., Moszkowicz, P., Gourdon, R., 2005. Effect of indigenous bacterial activity on arsenic mobilization under anaerobic conditions. Environ. Int., Recent Advances in Bioremediation 31, 221–226. https://doi.org/10.1016/j.envint.2004.09.019.

Coates, J.D., Ellis, D.J., Gaw, C.V., Lovley, D.R., 1999. Geothrix fermentans gen. nov., sp. nov., a novel Fe(III)-reducing bacterium from a hydrocarbon-contaminated aquifer. Int. J. Syst. Evol. Microbiol. 49, 1615–1622. https://doi.org/10.1099/00207713-49-4-1615.

Cutting, R.S., Coker, V.S., Fellowes, J.W., Lloyd, J.R., Vaughan, D.J., 2009. Mineralogical and morphological constraints on the reduction of Fe(III) minerals by Geobacter sulfurreducens. Geochem. Cosmochim. Acta 73, 4004–4022. https://doi.org/10.1016/j.gca.2009.04.009.

Dhar, R.K., Zheng, Y., Saltikov, C.W., Radloff, K.A., Mailloux, B.J., Ahmed, KaziM., van Geen, A., 2011. Microbes enhance mobility of arsenic in Pleistocene aquifer sand from Bangladesh. Environ. Sci. Technol. 45, 2648–2654. https://doi.org/10.1021/es1022015.

Dixit, S., Hering, J.G., 2003. Comparison of arsenic(V) and arsenic(III) sorption onto iron oxide minerals: implications for arsenic mobility. Environ. Sci. Technol. 37, 4182–4189. https://doi.org/10.1021/es030309t.

Dong, Y., Sanford, R.A., Chang, Y., McInerney, M.J., Fouke, B.W., 2017. Hematite reduction buffers acid generation and enhances nutrient uptake by a fermentative iron reducing bacterium, *Orenia metallireducens* strain Z6. Environ. Sci. Technol. 51, 232–242. https://doi.org/10.1021/acs.est.6b04126.

Dunlop, D.J., Özdemir, O., Kono, M., 2007. Magnetizations of rocks and minerals. Treatise Geophys 5, 277–336.

Eiche, E., Neumann, T., Berg, M., Weinman, B., van Geen, A., Norra, S., Berner, Z., Trang, P.T.K., Viet, P.H., Stüben, D., 2008. Geochemical processes underlying a sharp contrast in groundwater arsenic concentrations in a village on the Red River delta, Vietnam. Appl. Geochem., Arsenic in groundwaters of South-East Asia: With emphasis on Cambodia and Vietnam 23, 3143–3154. https://doi.org/10.1016/j.apgeochem.2008.06.023.

Emerson, D., Weiss, J.V., Megonigal, J.P., 1999. Iron-oxidizing bacteria are associated with ferric hydroxide precipitates (Fe-plaque) on the roots of wetland plants. Appl. Environ. Microbiol. 65, 2758–2761. https://doi.org/10.1128/AEM.65.6.2758-2761.1999.

Esther, J., Sukla, L.B., Pradhan, N., Panda, S., 2015. Fe (III) reduction strategies of dissimilatory iron reducing bacteria. Kor. J. Chem. Eng. 32, 1–14. https://doi.org/10.1007/s11814-014-0286-x.

Ettwig, K.F., Zhu, B., Speth, D., Keltjens, J.T., Jetten, M.S.M., Kartal, B., 2016. Archaea catalyze iron-dependent anaerobic oxidation of methane. Proc. Natl. Acad. Sci. Unit. States Am. 113, 12792–12796. https://doi.org/10.1073/pnas.1609534113.

Ewels, P.A., Peltzer, A., Fillinger, S., Patel, H., Alneberg, J., Wilm, A., Garcia, M.U., Di Tommaso, P., Nahnsen, S., 2020. The nf-core framework for community-curated bioinformatics pipelines. Nat. Biotechnol. 38, 276–278. https://doi.org/10.1038/s41587-020-0439-x.

Farquhar, M.L., Charnock, J.M., Livens, F.R., Vaughan, D.J., 2002. Mechanisms of arsenic uptake from aqueous solution by interaction with goethite, lepidocrocite, mackinawite, and Pyrite: an X-ray absorption spectroscopy study. Environ. Sci. Technol. 36, 1757–1762. https://doi.org/10.1021/es010216g.

Ferris, F.G., 2005. Biogeochemical properties of bacteriogenic iron oxides. Geomicrobiol. J. 22, 79–85. https://doi.org/10.1080/01490450590945861.

Fortin, D., Langley, S., 2005. Formation and occurrence of biogenic iron-rich minerals. Earth Sci. Rev. 72, 1–19. https://doi.org/10.1016/j.earscirev.2005.03.002.

Fortin, D., Ferris, F.G., Scott, S.D., 1998. Formation of Fe-silicates and Fe-oxides on bacterial surfaces in samples collected near hydrothermal vents on the Southern Explorer Ridge in the Northeast Pacific Ocean. Am. Mineral. 83, 1399–1408. https://doi.org/10.2138/am-1998-11-1229.

Fredrickson, J.K., Zachara, J.M., Kennedy, D.W., Dong, H., Onstott, T.C., Hinman, N.W., Li, S., 1998a. Biogenic iron mineralization accompanying the dissimilatory reduction of hydrous ferric oxide by a groundwater bacterium. Geochem. Cosmochim. Acta 62, 3239–3257. https://doi.org/10.1016/S0016-7037(98)00243-9.

Fredrickson, J.K., Zachara, J.M., Kennedy, D.W., Dong, H., Onstott, T.C., Hinman, N.W., Li, S., 1998b. Biogenic iron mineralization accompanying the dissimilatory reduction of hydrous ferric oxide by a groundwater bacterium. Geochem. Cosmochim. Acta 62, 3239–3257. https://doi.org/10.1016/S0016-7037(98)00243-9.

Fredrickson, J.K., Zachara, J.M., Kukkadapu, R.K., Gorby, Y.A., Smith, S.C., Brown, C.F., 2001. Biotransformation of Ni-substituted hydrous ferric oxide by an Fe(III)-Reducing bacterium. Environ. Sci. Technol. 35, 703–712. https://doi.org/10.1021/es001500v.

Gimenez, J., Martinez, M., Depablo, J., Rovira, M., Duro, L., 2007. Arsenic sorption onto natural hematite, magnetite, and goethite. J. Hazard Mater. 141, 575–580. https://doi.org/10.1016/j.jhazmat.2006.07.020.

Glodowska, Stopelli, E., Schneider, M., Lightfoot, A., Rathi, B., Straub, D., Patzner, M., Duyen, V.T., Members, A.T., Berg, M., 2020a. Role of in situ natural organic matter in mobilizing as during microbial reduction of FeIII-Mineral-Bearing aquifer sediments from Hanoi (Vietnam). Environ. Sci. Technol. 54, 4149–4159.

Glodowska, Stopelli, E., Schneider, M., Rathi, B., Straub, D., Lightfoot, A., Kipfer, R., Berg, M., Jetten, M., Kleindienst, S., Kappler, A., 2020b. Arsenic mobilization by anaerobic iron-dependent methane oxidation. Commun. Earth Environ. 1, 1–7. https://doi.org/10.1038/s43247-020-00037-y.

Glodowska, Stopelli, E., Straub, D., Vu Thi, D., Trang, P.T.K., Viet, P.H., , AdvectAs team members, Berg, M., Kappler, A., Kleindienst, S., 2020c. Arsenic behavior in groundwater in Hanoi (Vietnam) influenced by a complex biogeochemical network of iron, methane, and sulfur cycling. J. Hazard Mater. 124398 https://doi.org/10.1016/j.jhazmat.2020.124398.

Grafe, M., Eick, M.J., Grossl, P.R., 2001. Adsorption of arsenate (V) and arsenite (III) on goethite in the presence and absence of dissolved organic carbon. Soil Sci. Soc. Am. J. 65, 1680–1687. https://doi.org/10.2136/sssaj2001.1680.

Grafe, M., Eick, M.J., Grossl, P.R., Saunders, A.M., 2002. Adsorption of arsenate and arsenite on ferrihydrite in the presence and absence of dissolved organic carbon. J. Environ. Qual. 31, 1115–1123. https://doi.org/10.2134/jeq2002.1115.

Gupta, M., Velayutham, P., Elbeshbishy, E., Hafez, H., Khafipour, E., Derakhshani, H., El Naggar, M.H., Levin, D.B., Nakhla, G., 2014. Co-fermentation of glucose, starch, and cellulose for mesophilic biohydrogen production. Int. J. Hydrogen Energy 39, 20958–20967. https://doi.org/10.1016/j.ijhydene.2014.10.079.

Hanna, K., 2007. Adsorption of aromatic carboxylate compounds on the surface of synthesized iron oxide-coated sands. Appl. Geochem. 22, 2045–2053. https://doi.org/10.1016/j.apgeochem.2007.05.005.

Hansel, C.M., Benner, S.G., Fendorf, S., 2005. Competing Fe(II)-Induced mineralization pathways of ferrihydrite. Environ. Sci. Technol. 39, 7147–7153. https://doi.org/10.1021/es050666z.

Hao, L., Guo, Y., Byrne, J.M., Zeitvogel, F., Schmid, G., Ingino, P., Li, J., Neu, T.R., Swanner, E.D., Kappler, A., Obst, M., 2016. Binding of heavy metal ions in aggregates of microbial cells, EPS and biogenic iron minerals measured in-situ using metal- and glycoconjugates-specific fluorophores. Geochem. Cosmochim. Acta 180, 66–96. https://doi.org/10.1016/j.gca.2016.02.016.

Hegler, F., Posth, N.R., Jiang, J., Kappler, A., 2008. Physiology of phototrophic iron(II)-oxidizing bacteria: implications for modern and ancient environments. FEMS Microbiol. Ecol. 66, 250–260. https://doi.org/10.1111/j.1574-6941.2008.00592.x.

Héry, M., Gault, A.G., Rowland, H.A.L., Lear, G., Polya, D.A., Lloyd, J.R., 2008.

Molecular and cultivation-dependent analysis of metal-reducing bacteria implicated in arsenic mobilisation in south-east asian aquifers. Appl. Geochem., Arsenic in groundwaters of South-East Asia: With emphasis on Cambodia and Vietnam 23, 3215–3223. https://doi.org/10.1016/j.apgeochem.2008.07.003.
Hohmann, C., Winkler, E., Morin, G., Kappler, A., 2010. Anaerobic Fe(II)-Oxidizing bacteria show as resistance and immobilize as during Fe(III) mineral precipitation. Environ. Sci. Technol. 44, 94–101. https://doi.org/10.1021/es900708s.
Islam, F.S., Gault, A.G., Boothman, C., Polya, D.A., Charnock, J.M., Chatterjee, D., Lloyd, J.R., 2004. Role of metal-reducing bacteria in arsenic release from Bengal delta sediments. Nature 430, 68–71. https://doi.org/10.1038/nature02638.
Islam, F.S., Boothman, C., Gault, A.G., Polya, D.A., Lloyd, J.R., 2005a. Potential role of the Fe(III)-reducing bacteria Geobacter and Geothrix in controlling arsenic solubility in Bengal delta sediments. Mineral. Mag. 69, 865–875. https://doi.org/10.1180/0026461056950294.
Islam, F.S., Pederick, R.L., Gault, A.G., Adams, L.K., Polya, D.A., Charnock, J.M., Lloyd, J.R., 2005b. Interactions between the Fe(III)-Reducing bacterium geobacter sulfurreducens and arsenate, and capture of the metalloid by biogenic Fe(II). Appl. Environ. Microbiol. 71, 8642–8648. https://doi.org/10.1128/AEM.71.12.8642-8648.2005.
Kampmann, K., Ratering, S., Kramer, I., Schmidt, M., Zerr, W., Schnell, S., 2012. Unexpected stability of Bacteroidetes and Firmicutes communities in laboratory biogas reactors fed with different defined substrates. Appl. Environ. Microbiol. 78, 2106–2119. https://doi.org/10.1128/AEM.06394-11.
Kappler, A., Newman, D.K., 2004. Formation of Fe(III)-minerals by Fe(II)-oxidizing photoautotrophic bacteria 11Associate editor. L. G. Benning. Geochim. Cosmochim. Acta 68, 1217–1226. https://doi.org/10.1016/j.gca.2003.09.006.
Kappler, A., Schink, B., Newman, D.K., 2005. Fe(III) mineral formation and cell encrustation by the nitrate-dependent Fe(II)-oxidizer strain BoFeN1. Geobiology 3, 235–245. https://doi.org/10.1111/j.1472-4669.2006.00056.x.
Kappler, A., Bryce, C., Mansor, M., Lueder, U., Byrne, J.M., Swanner, E.D., 2021. An evolving view on biogeochemical cycling of iron. Nat. Rev. Microbiol. 1–15. https://doi.org/10.1038/s41579-020-00502-7.
Karlin, R., 1990. Magnetite diagenesis in marine sediments from the Oregon continental margin. J. Geophys. Res. Solid Earth 95, 4405–4419. https://doi.org/10.1029/JB095iB04p04405.
Kiskira, K., Papirio, S., Mascolo, M.C., Fourdrin, C., Pechaud, Y., van Hullebusch, E.D., Esposito, G., 2019. Mineral characterization of the biogenic Fe(III)(hydr)oxides produced during Fe(II)-driven denitrification with Cu, Ni and Zn. Sci. Total Environ. 687, 401–412. https://doi.org/10.1016/j.scitotenv.2019.06.107.
Kleinert, S., Muehe, E.M., Posth, N.R., Dippon, U., Daus, B., Kappler, A., 2011. Biogenic Fe(III) minerals lower the efficiency of iron-mineral-based commercial filter systems for arsenic removal. Environ. Sci. Technol. 45, 7533–7541. https://doi.org/10.1021/es201522n.
Klueglein, N., Lösekann-Behrens, T., Obst, M., Behrens, S., Appel, E., Kappler, A., 2013. magnetite formation by the novel Fe(III)-reducing Geothrix fermentans strain HradG1 isolated from a hydrocarbon-contaminated sediment with increased magnetic susceptibility. Geomicrobiol. J. 30, 863–873. https://doi.org/10.1080/01490451.2013.790922.
Kontny, A., Schneider, M., Eiche, E., Stopelli, E., Glodowska, M., Rathi, B., Göttlicher, J., Byrne, J.M., Kappler, A., Berg, M., Vu Thi, D., Trang, P.T.K., Viet, P.H., Neumann, T., 2021. Iron mineral transformations and their impact on as (im) mobilization at redox interfaces in As-contaminated aquifers. Geochem. Cosmochim. Acta. https://doi.org/10.1016/j.gca.2020.12.029.
Langley, S., Gault, A., Ibrahim, A., Renaud, R., Fortin, D., Clark, I.D., Ferris, F.G., 2009. A comparison of the rates of Fe(III) reduction in synthetic and bacteriogenic iron oxides by *Shewanella putrefaciens* CN32. Geomicrobiol. J. 26, 57–70. https://doi.org/10.1080/01490450802674905.
Lenoble, V., Chabroullet, C., al Shukry, R., Serpaud, B., Deluchat, V., Bollinger, J.-C., 2004. Dynamic arsenic removal on a MnO2-loaded resin. J. Colloid Interface Sci. 280, 62–67. https://doi.org/10.1016/j.jcis.2004.07.034.
Li, H., Peng, J., 2011. [Phylogenetic diversity of dissimilatory Fe(III)-reducing bacteria in paddy soil]. Ying Yong Sheng Tai Xue Bao J. Appl. Ecol. 22, 2705–2710.
Lovley, D.R., Phillips, E.J.P., Lonergan, D.J., 1991. Enzymic versus nonenzymic mechanisms for iron(III) reduction in aquatic sediments. Environ. Sci. Technol. 25, 1062–1067. https://doi.org/10.1021/es00018a007.
Lueders, T., Manefield, M., Friedrich, M.W., 2004. Enhanced sensitivity of DNA- and rRNA-based stable isotope probing by fractionation and quantitative analysis of isopycnic centrifugation gradients. Environ. Microbiol. 6, 73–78. https://doi.org/10.1046/j.1462-2920.2003.00536.x.
Mandal, B.K., Suzuki, K.T., 2002. Arsenic round the world: a review. Talanta 58, 201–235. https://doi.org/10.1016/S0039-9140(02)00268-0.
Manning, B.A., Fendorf, S.E., Goldberg, S., 1998. Surface structures and stability of arsenic(III) on Goethite: spectroscopic evidence for inner-sphere complexes. Environ. Sci. Technol. 32, 2383–2388. https://doi.org/10.1021/es9802201.
Martin, M., 2011. Cutadapt removes adapter sequences from high-throughput sequencing reads. EMBnet.journal 17, 10–12. https://doi.org/10.14806/ej.17.1.200.
Miot, J., Benzerara, K., Morin, G., Kappler, A., Bernard, S., Obst, M., Férard, C., Skouri-Panet, F., Guigner, J.-M., Posth, N., Galvez, M., Brown, G.E., Guyot, F., 2009. Iron biomineralization by anaerobic neutrophilic iron-oxidizing bacteria. Geochem. Cosmochim. Acta 73, 696–711. https://doi.org/10.1016/j.gca.2008.10.033.
Molin, M., Ulven, S.M., Meltzer, H.M., Alexander, J., 2015. Arsenic in the human food chain, biotransformation and toxicology – review focusing on seafood arsenic. J. Trace Elem. Med. Biol., Special Section: 10th Nordic Symposium on Trace Elements in Human Health and Disease 31, 249–259. https://doi.org/10.1016/j.jtemb.2015.01.010.
Muehe, E.M., Kappler, A., 2014. Arsenic mobility and toxicity in South and Southeast Asia – a review on biogeochemistry, health and socio-economic effects, remediation and risk predictions. Environ. Chem. 11, 483–495. https://doi.org/10.1071/EN13230.
Muehe, E.M., Obst, M., Hitchcock, A., Tyliszczak, T., Behrens, S., Schröder, C., Byrne, J.M., Michel, F.M., Krämer, U., Kappler, A., 2013a. Fate of Cd during microbial Fe(III) mineral reduction by a novel and Cd-tolerant geobacter species. Environ. Sci. Technol. 47, 14099–14109. https://doi.org/10.1021/es403365w.
Muehe, E.M., Scheer, L., Daus, B., Kappler, A., 2013b. Fate of arsenic during microbial reduction of biogenic versus abiogenic as–Fe(III)–Mineral coprecipitates. Environ. Sci. Technol. 47, 8297–8307. https://doi.org/10.1021/es400801z.
Muehe, E.M., Morin, G., Scheer, L., Pape, P.L., Esteve, I., Daus, B., Kappler, A., 2016. Arsenic(V) incorporation in vivianite during microbial reduction of arsenic(V)-Bearing biogenic Fe(III) (Oxyhydr)oxides. Environ. Sci. Technol. 50, 2281–2291. https://doi.org/10.1021/acs.est.5b04625.
Muhammad, S., Tahir Shah, M., Khan, S., 2010. Arsenic health risk assessment in drinking water and source apportionment using multivariate statistical techniques in Kohistan region, northern Pakistan. Food Chem. Toxicol. 48, 2855–2864. https://doi.org/10.1016/j.fct.2010.07.018.
National Research Council, 2001. Arsenic in Drinking Water: 2001 Update.
Neidhardt, H., Winkel, L.H.E., Kaegi, R., Stengel, C., Trang, P.T.K., Lan, V.M., Viet, P.H., Berg, M., 2018. Insights into arsenic retention dynamics of Pleistocene aquifer sediments by in situ sorption experiments. Water Res. 129, 123–132. https://doi.org/10.1016/j.watres.2017.11.018.
Neumann, R.B., Pracht, L.E., Polizzotto, M.L., Badruzzaman, A.B.M., Ali, M.A., 2014. Biodegradable organic carbon in sediments of an arsenic-contaminated aquifer in Bangladesh. Environ. Sci. Technol. Lett. 1, 221–225. https://doi.org/10.1021/ez5000644.
Ona-Nguema, G., Morin, G., Juillot, F., Calas, G., Brown, G.E., 2005. EXAFS analysis of arsenite adsorption onto two-line ferrihydrite, hematite, goethite, and lepidocrocite. Environ. Sci. Technol. 39, 9147–9155. https://doi.org/10.1021/es050889p.
Oremland, R.S., Stolz, J.F., 2003. The ecology of arsenic. Science 300, 939–944. https://doi.org/10.1126/science.1081903.
Parada, A.E., Needham, D.M., Fuhrman, J.A., 2016. Every base matters: assessing small subunit rRNA primers for marine microbiomes with mock communities, time series and global field samples. Environ. Microbiol. 18, 1403–1414. https://doi.org/10.1111/1462-2920.13023.
Pérez-Rodríguez, I., Rawls, M., Coykendall, D.K., Foustoukos, D.I., 2016. Deferrisoma palaeochoriense sp. nov., a thermophilic, iron(III)-reducing bacterium from a shallow-water hydrothermal vent in the Mediterranean Sea. Int. J. Syst. Evol. Microbiol. 66, 830–836. https://doi.org/10.1099/ijsem.0.000798.
Petrusevski, B., Sharma, S., Schippers, J., Shordt, K., 2007. Arsenic in Drinking Water.
Podgorski, J., Berg, M., 2020. Global threat of arsenic in groundwater. Science 368, 845–850. https://doi.org/10.1126/science.aba1510.
Posth, N.R., Huelin, S., Konhauser, K.O., Kappler, A., 2010. Size, density and composition of cell–mineral aggregates formed during anoxygenic phototrophic Fe(II) oxidation: impact on modern and ancient environments. Geochem. Cosmochim. Acta 74, 3476–3493. https://doi.org/10.1016/j.gca.2010.02.036.
Posth, N.R., Canfield, D.E., Kappler, A., 2014. Biogenic Fe(III) minerals: from formation to diagenesis and preservation in the rock record. Earth Sci. Rev. 135, 103–121. https://doi.org/10.1016/j.earscirev.2014.03.012.
Postma, D., Mai, N.T.H., Lan, V.M., Trang, P.T.K., Sø, H.U., Nhan, P.Q., Larsen, F., Viet, P.H., Jakobsen, R., 2017. Fate of arsenic during red river water infiltration into aquifers beneath Hanoi, Vietnam. Environ. Sci. Technol. 51, 838–845. https://doi.org/10.1021/acs.est.6b05065.
Pruesse, E., Quast, C., Knittel, K., Fuchs, B.M., Ludwig, W., Peplies, J., Glöckner, F.O., 2007. SILVA: a comprehensive online resource for quality checked and aligned ribosomal RNA sequence data compatible with ARB. Nucleic Acids Res. 35, 7188–7196. https://doi.org/10.1093/nar/gkm864.
Qi, P., Pichler, T., 2014. Closer look at as(III) and as(V) adsorption onto ferrihydrite under competitive conditions. Langmuir 30, 11110–11116. https://doi.org/10.1021/la502740w.
Rajput, S., Pittman, C.U., Mohan, D., 2016. Magnetic magnetite (Fe3O4) nanoparticle synthesis and applications for lead (Pb2+) and chromium (Cr6+) removal from water. J. Colloid Interface Sci. 468, 334–346. https://doi.org/10.1016/j.jcis.2015.12.008.
Roden, E.E., 2004. Analysis of long-term bacterial vs. chemical Fe(III) oxide reduction kinetics. Geochem. Cosmochim. Acta 68, 3205–3216. https://doi.org/10.1016/j.gca.2004.03.028.
Schädler, S., Burkhardt, C., Hegler, F., Straub, K.L., Miot, J., Benzerara, K., Kappler, A., 2009. formation of cell-iron-mineral aggregates by phototrophic and nitrate-reducing anaerobic Fe(II)-Oxidizing bacteria. Geomicrobiol. J. 26, 93–103. https://doi.org/10.1080/01490450802660573.
Scheidegger, A., Borkovec, M., Sticher, H., 1993. Coating of silica sand with goethite: preparation and analytical identification. Geoderma 58, 43–65. https://doi.org/10.1016/0016-7061(93)90084-X.
Schwertmann, U., Cornell, R.M., 2008. Iron Oxides in the Laboratory: Preparation and Characterization. John Wiley & Sons.
Shen, L., Ouyang, L., Zhu, Y., Trimmer, M., 2019. Active pathways of anaerobic methane oxidation across contrasting riverbeds. ISME J. 13, 752–766. https://doi.org/10.1038/s41396-018-0302-y.
Slobodkina, G.B., Reysenbach, A.-L., Panteleeva, A.N., Kostrikina, N.A., Wagner, I.D.,

Bonch-Osmolovskaya, E.A., Slobodkin, A.I., 2012. Deferrisoma camini gen. nov., sp. nov., a moderately thermophilic, dissimilatory iron(III)-reducing bacterium from a deep-sea hydrothermal vent that forms a distinct phylogenetic branch in the Deltaproteobacteria. Int. J. Syst. Evol. Microbiol. 62, 2463–2468. https://doi.org/10.1099/ijs.0.038372-0.

Smedley, P.L., Kinniburgh, D.G., 2002. A review of the source, behaviour and distribution of arsenic in natural waters. Appl. Geochem. 17, 517–568. https://doi.org/10.1016/S0883-2927(02)00018-5.

Sorwat, J., Mellage, A., Kappler, A., Byrne, J.M., 2020. Immobilizing magnetite onto quartz sand for chromium remediation. J. Hazard Mater. 400, 123139. https://doi.org/10.1016/j.jhazmat.2020.123139.

Stollenwerk, K.G., Breit, G.N., Welch, A.H., Yount, J.C., Whitney, J.W., Foster, A.L., Uddin, M.N., Majumder, R.K., Ahmed, N., 2007. Arsenic attenuation by oxidized aquifer sediments in Bangladesh. Sci. Total Environ., Arsenic in the Environment: Biology and Chemistry 379, 133–150. https://doi.org/10.1016/j.scitotenv.2006.11.029.

Stopelli, E., Duyen, V.T., Mai, T.T., Trang, P.T.K., Viet, P.H., Lightfoot, A., Kipfer, R., Schneider, M., Eiche, E., Kontny, A., Neumann, T., Glodowska, M., Patzner, M., Kappler, A., Kleindienst, S., Rathi, B., Cirpka, O., Bostick, B., Prommer, H., Winkel, L.H.E., Berg, M., 2020. Spatial and temporal evolution of groundwater arsenic contamination in the Red River delta, Vietnam: interplay of mobilisation and retardation processes. Sci. Total Environ. 717, 137143. https://doi.org/10.1016/j.scitotenv.2020.137143.

Straub, D., Blackwell, N., Langarica-Fuentes, A., Peltzer, A., Nahnsen, S., Kleindienst, S., 2020. Interpretations of environmental microbial community studies are biased by the selected 16S rRNA (gene) amplicon sequencing pipeline. Front. Microbiol. 11 https://doi.org/10.3389/fmicb.2020.550420.

Tan, J., Wang, J., Xue, J., Liu, S.-Y., Peng, S.-C., Ma, D., Chen, T.-H., Yue, Z., 2015. Methane production and microbial community analysis in the goethite facilitated anaerobic reactors using algal biomass. Fuel 145, 196–201. https://doi.org/10.1016/j.fuel.2014.12.087.

Treude, N., Rosencrantz, D., Liesack, W., Schnell, S., 2003. Strain FAc12, a dissimilatory iron-reducing member of the Anaeromyxobacter subgroup of Myxococcales. FEMS Microbiol. Ecol. 44, 261–269. https://doi.org/10.1016/S0168-6496(03)00048-5.

Ueshima, M., Tazaki, K., 2001. Possible role of microbial polysaccharides in nontronite formation. Clay Clay Miner. 49, 292–299. https://doi.org/10.1346/CCMN.2001.0490403.

van Geen, A., Bostick, B.C., Thi Kim Trang, P., Lan, V.M., Mai, N.-N., Manh, P.D., Viet, P.H., Radloff, K., Aziz, Z., Mey, J.L., Stahl, M.O., Harvey, C.F., Oates, P., Weinman, B., Stengel, C., Frei, F., Kipfer, R., Berg, M., 2013. Retardation of arsenic transport through a Pleistocene aquifer. Nature 501, 204–207. https://doi.org/10.1038/nature12444.

Voegelin, A., Kaegi, R., Frommer, J., Vantelon, D., Hug, S.J., 2010. Effect of phosphate, silicate, and Ca on Fe(III)-precipitates formed in aerated Fe(II)- and As(III)-containing water studied by X-ray absorption spectroscopy. Geochem. Cosmochim. Acta 74, 164–186. https://doi.org/10.1016/j.gca.2009.09.020.

Wallis, I., Prommer, H., Berg, M., Siade, A.J., Sun, J., Kipfer, R., 2020. The river–groundwater interface as a hotspot for arsenic release. Nat. Geosci. 13, 288–295. https://doi.org/10.1038/s41561-020-0557-6.

Wang, R., Xu, S.-Y., Zhang, M., Ghulam, A., Dai, C.-L., Zheng, P., 2020. Iron as electron donor for denitrification: the efficiency, toxicity and mechanism. Ecotoxicol. Environ. Saf. 194, 110343. https://doi.org/10.1016/j.ecoenv.2020.110343.

Welch, A.H., Westjohn, D.B., Helsel, D.R., Wanty, R.B., 2000. Arsenic in ground water of the United States: occurrence and geochemistry. Groundwater 38, 589–604. https://doi.org/10.1111/j.1745-6584.2000.tb00251.x.

Zachara, J.M., Fredrickson, J.K., Li, S.-M., Kennedy, D.W., Smith, S.C., Gassman, P.L., 1998. Bacterial reduction of crystalline Fe (super 3+) oxides in single phase suspensions and subsurface materials. Am. Mineral. 83, 1426–1443. https://doi.org/10.2138/am-1998-11-1232.

Zachara, J.M., Kukkadapu, R.K., Fredrickson, J.K., Gorby, Y.A., Smith, S.C., 2002. Biomineralization of poorly crystalline Fe(III) oxides by dissimilatory metal reducing bacteria (DMRB). Geomicrobiol. J. 19, 179–207. https://doi.org/10.1080/01490450252864271.

Zhang, H., Liu, F., Zheng, S., Chen, L., Zhang, X., Gong, J., 2020. The differentiation of iron-reducing bacterial community and iron-reduction activity between riverine and marine sediments in the Yellow River estuary. Mar. Life Sci. Technol. 2, 87–96. https://doi.org/10.1007/s42995-019-00001-6.

Zhao, Zisheng, Li, Y., Zhao, Zhiqiang, Yu, Q., Zhang, Y., 2020. Effects of dissimilatory iron reduction on acetate production from the anaerobic fermentation of waste activated sludge under alkaline conditions. Environ. Res. 182, 109045. https://doi.org/10.1016/j.envres.2019.109045.

Glodowska, M., Schneider, M., Eiche, E., Kontny, A., Neumann, T., Straub, D., Berg, M., Prommer, H., Bostick, B.C., Nghiem, A.A., Schneider, M., 2021. Fermentation, methanotrophy and methanogenesis influence sedimentary Fe and As dynamics in As-affected aquifers in Vietnam. Sci. Total Environ. 146501. https://doi.org/10.1016/j.scitotenv.2021.146501.